**Civil Engineering and Applied Solutions**

*Research Article*

journal homepage: ceas.journals.umz.ac.ir

CEAS Civil Engineering and Applied Solutions

# Influence of Near-Fault Unidirectional and Bidirectional Ground Motions on DSM-Enhanced Reactor Building Foundations Considering Soil–Structure Interaction: A Case Study

Ali Yaghfoori [a], Iradj Mahmoudzadeh Kani [a*], Hassan Yousefi [a]

[a] *School of Civil Engineering, College of Engineering, University of Tehran, Tehran, Iran*

ARTICLE INFO

*Keywords:*
Finite-element modelling
Deep soil mixing
Multidirectional Loading
Rocking motion
Nuclear power plant

*Article history:*
Received 13 December 2025
Accepted 31 January 2026
Available online 01 July 2026

ABSTRACT

This study examines the seismic performance of the APR1400 nuclear reactor, focusing on soil–structure interaction (SSI) and structure–soil–structure interaction (SSSI), particularly on foundations enhanced with block deep soil mixing (DSM). The reactor, including its internal structure, containment building, and DSM layers, was modeled to evaluate its dynamic response to unidirectional and bidirectional near-fault ground motions with different frequency contents. Results indicate that the internal structure experiences higher horizontal accelerations than the containment building, while rocking-induced vertical accelerations are significant in the containment. DSM effectiveness depends on the frequency content of the ground motion, soil properties, and DSM depth. Horizontal accelerations are largely unaffected at high frequencies, but low-frequency responses are notably reduced. In the vertical component, accelerations in the 2–10 Hz range increase by over 140% in the containment building and nearly 60% in the internal structure for an 18-m DSM layer, highlighting the vulnerability of many reactor components. Morlet wavelet analysis shows that DSM reduces horizontal-acceleration energy transmitted to the containment building while shifting it to higher frequencies. In contrast, vertical-acceleration energy is substantially amplified, particularly in the 3–7 Hz range. SSSI effects significantly influence structural response: for modeling a second reactor at a 30-m distance, horizontal energy decreases by approximately 34% in the internal structure, while vertical acceleration energy increases by 3.2 times; at 70-m spacing, vertical energy rises by up to 8 times. Bidirectional near-fault excitations further increase vertical accelerations by 6–46 times compared to unidirectional loading, depending on the structure and earthquake. These findings underscore the critical importance of accounting for multidirectional excitations, DSM-induced effects, and SSSI in the seismic design of nuclear facilities, particularly for sensitive equipment and high-frequency structural responses. Accurate evaluation of these factors is essential to ensure operational safety and prevent potential damage to reactor components under severe near-fault ground motions.

## 1. Introduction

Several ground-motion characteristics, including Ground Motion Incoherency (GMI), Peak Ground Acceleration (PGA), and frequency content (FC), significantly affect the seismic response of nuclear power plant (NPP) structures [1]. These factors must be meticulously evaluated in Soil-Structure Interaction (SSI) analyses. At a power plant site, various structures with differing weights, volumes, sizes, and foundation depths may sit on individual or combined foundations. Given the heightened sensitivity of these

* Corresponding author.
*E-mail addresses:* imkani@ut.ac.ir (I. Mahmoudzadeh Kani).

https://doi.org/10.22080/ceas.2026.30778.1064
**ISSN:** 3092-7749/
How to cite this article: Yaghfoori, A., Mahmoudzadeh Kani, I., Yousefi, H. Influence of Near-Fault Unidirectional and Bidirectional Ground Motions on DSM-Enhanced Reactor Building Foundations Considering Soil–Structure Interaction: A Case Study. Civil Engineering and Applied Solutions. 2026; 2(3): 49–72. doi.org/10.22080/ceas.2026.30778.1064.

structures, particularly their equipment, it is crucial to account for soil–structure interaction (SSI) and thoroughly investigate its effects [2]. Kitada et al. [3-5] demonstrated through laboratory studies, numerical analyses, and the construction of large-scale power plant structures that soil properties influence the seismic performance of each structure, the arrangement of adjacent structures, their dynamic characteristics, the direction of earthquake loading, and other factors. They also showed that thin soil layers can alter the seismic behaviour of structures and that heavy structures, such as reactors, can significantly affect neighbouring structures, including turbines. Clouteau et al. [6] investigated the effect of structure–soil–structure interaction (SSSI) and showed that the presence of a second building, compared to a single building, has little influence on the response of both buildings with surface foundations; however, this influence can be more significant when embedded foundations are used. Roy et al. [7] studied the effects of soil-structure-soil interaction (SSSI). Their findings show that nearby structures significantly influence a structure's dynamic response, depending on proximity, soil type, and foundation conditions. Heavy structures impact the surrounding soil motion, but transferring this motion to the free field is complex. SSSI effects amplify responses in closely spaced heavy structures, with the greatest increases in stiff soils, short spacing, and deep embedment; peak response accelerations can exceed 3.5 times. These effects lessen with lower soil stiffness, greater distance, and shallower embedment. Given the complexity, each case should be examined individually. Lee and Lee and Wesley [8] investigated highly simplified structural models and demonstrated that interaction between adjacent structures can significantly affect the dynamic response of a wide range of structures. These effects are particularly pronounced in large-scale facilities such as nuclear power plants, and the intensity of structure–soil–structure interaction (SSSI) increases when the structures are founded on soil deposits other than hard rock. Bolisetti and Whittaker [9] investigated the effects of structure–soil–structure interaction (SSSI) by considering the mass and separation distance between nuclear plant structures. Their findings indicated that SSSI effects are most pronounced within the reactors' rocking-frequency range. Moreover, when there is a substantial mass difference between adjacent structures, the intensity of these interactions increases. However, a fourfold increase in the mass of both adjacent reactors did not produce a discernible change in their seismic response. Yue et al. [10] assessed the effects of structure-soil-structure interaction (SSSI) on two nuclear power plant buildings with embedded foundations. The results showed that the lighter turbine building has a minimal impact on the seismic response of the nearby reactor building. These results support the prevailing notion that heavier structures within the nuclear island can influence the seismic behaviour of surrounding lighter buildings. Anderson et al. [11] investigated the effects of earthquake characteristics, soil, and structure on the structure-soil-structure interaction (SSSI) of power plant buildings. The results showed that the Pretreatment Facility Control Building experiences a significant increase in seismic demand due to interaction with a larger adjacent structure. Anderson et al. [11] indicated that the influence of structure–soil–structure interaction (SSSI) can be disregarded for bedrock sites, while it should be considered for non-bedrock sites. Nonetheless, these findings highlight that the SSSI mechanism among neighbouring structures in nuclear power plants is exceptionally intricate, with effects that vary from case to case, necessitating careful evaluation in each instance. Using advanced numerical modelling, Kanellopoulos et al. [12] studied a nuclear power plant's structure–soil–structure interaction (SSSI). Results indicated that elastic soil and the absence of auxiliary buildings enable soil–structure interaction to produce an additional rocking-type vibration mode that is undetectable by fixed-base models. Thus, neglecting the SSI effect is not always correct. The presence of the auxiliary building increases the spectral acceleration of the reactor building, especially at the auxiliary building's resonance frequency. SSSI effects can be beneficial or detrimental, depending on structural characteristics and site conditions, and vary by configuration. They recommended that design engineers enhance the accuracy and complexity of their modelling for analysing SSSI effects in nuclear power plants. Block-type Deep Soil Mixing (DSM) is often recommended to improve soil quality, particularly for sensitive and heavy structures such as power plant facilities. Shaghaghi et al. [13] examined the seismic behaviour of block-type Deep Soil Mixing (DSM) through fully nonlinear analyses. Their findings indicated that this method considerably decreases surface acceleration and enhances the seismic response of the soil layer. Yaghfoori et al. [14], in a case study on block deep mixing (BDM) implemented in an ongoing power plant project, reported that the BDM improvement system significantly reduces the horizontal acceleration transmitted to the DSM units, with the magnitude of this reduction increasing with DSM thickness. Conversely, the vertical acceleration associated with rocking motion increased with increasing depth of improvement. Based on their analyses, they recommended adopting one-quarter of the average shear wavelength in the soil as the optimal DSM depth. Furthermore, their findings indicated that the width of the DSM blocks had no significant effect on horizontal acceleration. However, increasing the block width effectively mitigates the vertical acceleration generated by rocking. They also observed that expanding the DSM width beyond 1.5 times its initial value does not yield additional improvement in controlling the rocking response. Although the block-type Deep Soil Mixing (DSM) technique has been recommended in practice and examined in previous engineering research as an effective ground improvement method for critical infrastructure, such as nuclear facilities, a thorough review of the literature indicates that very few studies have investigated the seismic behavior of this specific DSM configuration and its interaction with foundations and superstructures. Most prior studies have focused on other DSM arrangements, such as grid- or column-type patterns, primarily emphasizing their ability to mitigate liquefaction, rather than providing a comprehensive evaluation of their seismic performance. Therefore, the main novelty of this work lies in the systematic and thorough assessment of the seismic performance of block-type DSM and its soil–foundation–structure interaction (SFSI) through extensive time-domain and parametric analyses, based on laboratory and field results from an ongoing nuclear power plant project. In particular, given the large volume and significant stiffness contrast between block-type DSM and the surrounding soil, this study evaluates the rocking motion and associated vertical accelerations under both unidirectional and bidirectional earthquake loading. Furthermore, by incorporating free-field soil columns and Lysmer–Kuhlemeyer dashpots along the lateral and bottom boundaries, the model ensures realistic wave propagation and energy absorption at the model boundaries. Additionally, using Morlet power spectrum analysis, it is demonstrated that block-type DSM improvement can significantly affect the energy distribution of the structural acceleration response, highlighting a novel aspect of its dynamic behavior. Recent research has focused less on the seismic performance of DSM and its interaction with the soil, foundation, and superstructure. This study uses soil profiles derived from laboratory testing and field

investigations conducted as part of an ongoing power plant project to assess the seismic performance of the APR1400 reactor structure, with particular emphasis on soil-structure interaction. The site characteristics are described in detail based on comprehensive geotechnical investigations. Given that the project uses the block deep mixing (BDSM) method for ground improvement, the reactor structure and foundation are explicitly modeled, and the surrounding soil mass is improved through deep soil mixing (DSM). The soil-structure interaction effects are then analyzed under horizontal excitations induced by three earthquake records with varying frequency content. Finally, the influence of structure-soil-structure interaction is evaluated by modeling two reactor buildings at different spacings to investigate their coupled seismic response.

## 2. Model properties

### *2.1. Structural properties*

In this study, the seismic performance of the APR1400 nuclear reactor structure is investigated. The superstructure, comprising the containment building and internal structural components, is modelled on top of a foundation and ground improvement using the block-type deep soil mixing (DSM) method. The soil profile is stratified and defined based on site-specific geotechnical investigations. The modelled soil domain extends to a depth of 150 meters, with DSM treatment layers of 8 and 18 meters, respectively. The foundation is assumed to have a radius of 25 meters and a thickness of 3 meters. The containment and internal structures are idealized using equivalent stick-beam models with lumped masses to simplify the model and reduce computational costs (Fig. 1). Such modelling approaches are widely adopted in structural analyses of nuclear power plant facilities [15, 16]. Furthermore, relevant design codes and standards allow and acknowledge the use of this modelling technique for nuclear structures [17]. Tables 1 and 2 provide details of the lumped-mass stick models for the containment building and the internal structure, respectively. Implementing material damping in the frequency domain is relatively straightforward. However, in time-domain analyses, material damping must be approximated using Rayleigh damping. To define Rayleigh damping, the mass-proportional $\alpha$ and stiffness-proportional $\beta$ coefficients are calculated based on selected natural frequencies $\omega_n$ and $\omega_m$ corresponding to modes $m$ and $n$, along with the target damping ratio [15]. The expressions used to compute $\alpha$ and $\beta$ are as follows:

$$\alpha = \xi \frac{2\omega_m \omega_n}{\omega_m + \omega_n} \tag{1}$$

$$\beta = \xi \frac{2}{\omega_m + \omega_n} \tag{2}$$

The Rayleigh damping coefficients were determined based on the dominant frequencies of the coupled soil–foundation–superstructure system, including both soil- and structure-dominated modes. This approach ensures that the damping model accurately represents the system's dynamic behavior. The system transfer function and the corresponding dominant frequencies are shown in Fig. 2. Concrete is used for the superstructure. The material properties are presented in Table 3.

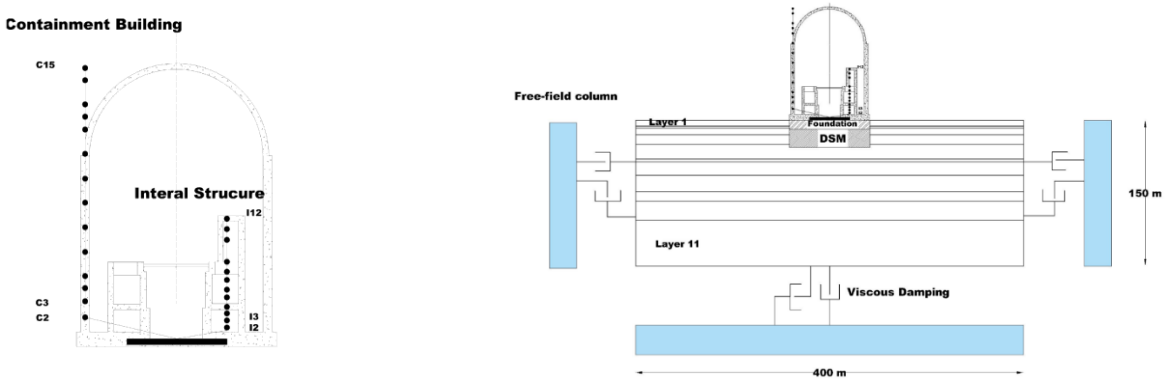


**Fig. 1. Soil structure system. (a) Stick beam; (b) Elevation view.**

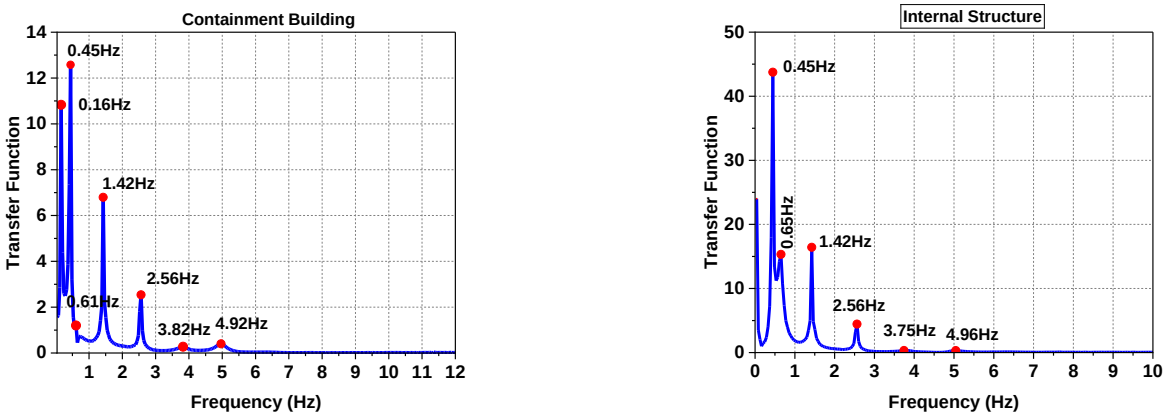


**Fig. 2. Transfer function of the internal structure and the containment building.**

**Table 1. Properties of a containment building.**

| Node-Containment building | Elevation (m) | Lumped mass (ton) | Connection node | Area ($m^2$) | Moment of inertia ($m^4$) | Torsional inertia ($m^4$) |
|---|---|---|---|---|---|---|
| 1 | 0 | 853.7 | - | - | - | - |
| 2 | 3.5 | 1633.1 | C1 -C2 | 202.9 | 56299.8 | 112634.2 |
| 3 | 7 | 1818.4 | C2-C3 | 202.9 | 56299.8 | 112634.2 |
| 4 | 11 | 1856.3 | C3-C4 | 202.9 | 56299.8 | 112634.2 |
| 5 | 14 | 1671 | C4-C5 | 202.9 | 56299.8 | 112634.2 |
| 6 | 18 | 2301.4 | C5-C6 | 202.9 | 56299.8 | 112634.2 |
| 7 | 24 | 3080.8 | C6-C7 | 202.9 | 56299.8 | 112634.2 |
| 8 | 30.5 | 3266.1 | C7-C8 | 202.9 | 56299.8 | 112634.2 |
| 9 | 37 | 3118.7 | C8-C9 | 202.9 | 56299.8 | 112634.2 |
| 10 | 44 | 3044.3 | C9-C10 | 202.9 | 56299.8 | 112634.2 |
| 11 | 50 | 3695.2 | C10-C11 | 202.9 | 56299.8 | 112634.2 |
| 12 | 54 | 2745.1 | C11-C12 | 202.9 | 56299.8 | 112634.2 |
| 13 | 62 | 3486.5 | C12-C13 | 179.8 | 47591.2 | 95199.7 |
| 14 | 70 | 3452.9 | C13-C14 | 179.8 | 35861.7 | 71732 |
| 15 | 78 | 1442.9 | C14-C15 | 166.1 | 12825.6 | 25651.3 |

**Table 2. Properties of internal structure.**

| Node-Internal Structure | Elevation (m) | Lumped mass (ton) | Connection node | Area ($m^2$) | Moment of inertia ($m^4$) | Torsional inertia ($m^4$) |
|---|---|---|---|---|---|---|
| 1 | 0 | 1806.1 | - | - | - | - |
| 2 | 1.5 | 3348 | I1-I2 | 833.2 | 79896.9 | 164989.7 |
| 3 | 3.5 | 7810.8 | I2-I3 | 884 | 81942.5 | 167389.1 |
| 4 | 7 | 5135.4 | I3-I4 | 857.9 | 80710.1 | 165957.8 |
| 5 | 9 | 2678.3 | I4-I5 | 313.8 | 21253.4 | 37753.4 |
| 6 | 11 | 2905.6 | I5-I6 | 254.6 | 19443.0 | 35811.7 |
| 7 | 14 | 2911.2 | I6-I7 | 221.9 | 19384.0 | 35233.9 |
| 8 | 16 | 3486 | I7-I8 | 261.4 | 20166.3 | 36571.3 |
| 9 | 18 | 789.5 | I8-I9 | 202.8 | 18524.1 | 34566.9 |
| 10 | 20 | 2595.2 | I9-I10 | 202.8 | 18524.1 | 34566.9 |
| 11 | 24 | 2507.4 | I10-I11 | 202.7 | 18524.1 | 34566.9 |
| 12 | 29.5 | 2665.1 | I11-I12 | 103.2 | 4666.7 | 7888.6 |
| 13 | 34.5 | 798.1 | I12-I13 | 97.9 | 4642.6 | 7840.4 |

**Table 3. Material properties of concrete.**

| Young's modulus ($kN/m^2$) | Poisson's ratio | Mass density ($t/m^3$) |
|---|---|---|
| $3.045\times10^7$ | 0.17 | 2.4 |

### *2.2. Soil properties*

This study examined a soil profile from a nuclear power plant project currently under construction. The engineering geological conditions of the site were assessed mainly through borehole drilling and test excavations, including soil pits. In total, 365 boreholes were drilled, achieving an accumulated depth of approximately 9,200 meters, with the maximum depth reaching 120 meters below the surface. Core drilling was conducted using various types of Mobil Drill rigs and different models of XY-series drilling machines, which are available in both electric and diesel versions. Based on geotechnical and geological field data assessments and laboratory tests on the soil's physical and mechanical properties, 14 unique Engineering Geological Elements (EGEs) were identified in the project area. The site's subsurface contains soil deposits extending to depths beyond 200 meters. This project included downhole investigations using the seismic logging method in 53 boreholes to evaluate the dynamic properties of the foundation soils. During these investigations, S-wave (Vs) and P-wave velocities were measured for each soil layer, and key dynamic parameters, including Poisson's ratio, shear modulus, Young's modulus, and bulk modulus, were calculated. In the study area, P-wave velocities range from 400 to 2700 m/s, while S-wave velocities (Vs) vary from 156 to 900 m/s. The highest Vs values (700–900 m/s) were observed in a high-velocity near-surface layer located 2-3 meters beneath the ground surface, with an average thickness of 5-6 meters. Below

this layer, soils with lower Vs values were detected. Generally, S-wave velocity increases with depth, reaching 660 m/s in certain boreholes. For instance, the shear wave velocity profiles for boreholes 167 and 176 are shown in Fig. 3. Ultimately, variations in soil characteristics with depth were modelled using an 11-layer horizontal approach based on average data from 365 boreholes of varying depths, as shown in Fig. 1 and detailed in Table 4.

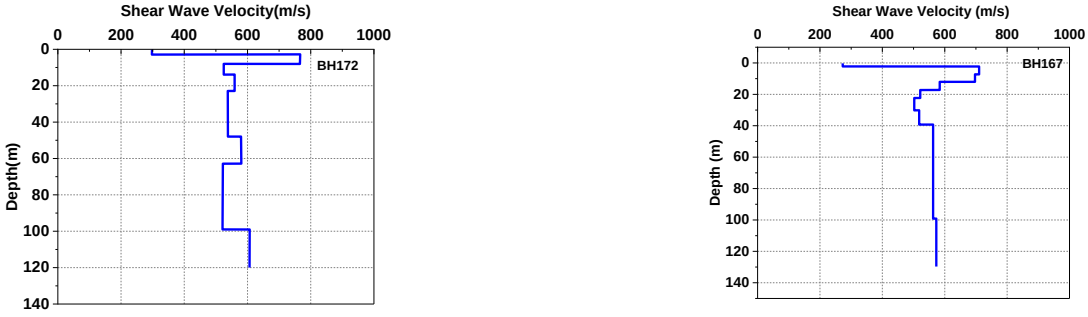


**(a)** **(b)**

**Fig. 3. Shear Wave Velocity Profiles of Boreholes, (a) Borehole 172; (b) Borehole 167.**

**Table 4. Properties of soil layers.**

| Layer | Thickness (m) | Depth (m) | Density (t/m$^3$) | S-Wave velocity (m/s) | P-Wave velocity (m/s) |
|---|---|---|---|---|---|
| 1 | 6 | 6 | 2.02 | 445.9 | 1777.1 |
| 2 | 2 | 8 | 2.02 | 385.6 | 1960 |
| 3 | 6.8 | 14.8 | 2.02 | 344.6 | 1960 |
| 4 | 9.9 | 24.7 | 2.008 | 297.8 | 1917.5 |
| 5 | 15 | 39.7 | 2 | 277.8 | 1890 |
| 6 | 3 | 42.7 | 2.03 | 430.2 | 2200 |
| 7 | 14 | 56.7 | 2.035 | 304.5 | 1660 |
| 8 | 17 | 73.7 | 2.028 | 354.8 | 2100 |
| 9 | 9.5 | 83.2 | 2.03 | 320 | 2100 |
| 10 | 19.5 | 102.7 | 2.03 | 317 | 2100 |
| 11 | 47.3 | 150 | 2 | 362.5 | 2100 |

### *2.3. Block deep soil mixing properties*

Six boreholes were drilled at the site to facilitate the design of Deep Soil Mixing (DSM) columns, and 900 kg of soil samples were collected for laboratory analysis. The tests were designed to assess the behaviour of soil-cement samples considering different soil layers, cement types, curing durations, and cement quantities, with a particular emphasis on determining the total water-to-cement ratio and the water-to-cement ratio of the cement slurry. The primary criterion for selecting the optimal mixing parameters was compressive strength. Four curing durations were evaluated: 7, 14, 28, and 56 days. The initial four chosen values for the total water-to-cement ratio ($W_T$: C) were 1.7, 2, 2.5, and 3. Given that the anticipated service life of the DSM columns exceeds 80 years, it was essential to consider the potentially aggressive groundwater chemistry. Two cement types, Type II and Type V, as defined in ASTM C150, were employed to address this concern. Based on the laboratory findings, Fig. 4 illustrates the unconfined compressive strength values for various total water-to-cement ratios using Type II and Type V cement.

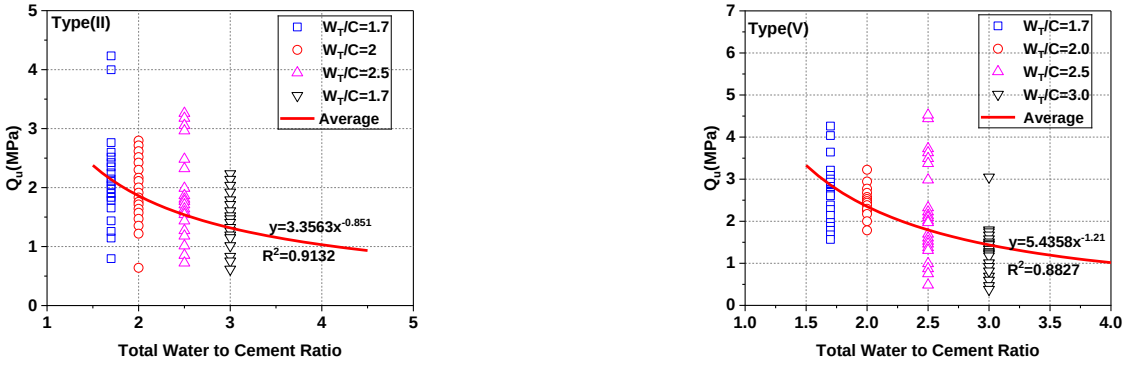


**(a)** **(b)**

**Fig. 4. $Q_u$ as a function of total water-to-cement ratio, (a) Type II cement; (b) Type V cement.**

The target parameters for the DSM columns were established based on laboratory test outcomes. The water-to-slurry ratio was fixed at 1, while the total water-to-cement ratio was set at 1.7. Laboratory results showed that Type I and Type V cement met the soil's sulfate conditions. However, Type V cement was chosen due to its lower water-to-cement ratio requirement, which enhances strength. The overlap for the deep mixing columns was 20%, and the columns had a diameter of 1.6 meters. To assess and optimize factors affecting column construction, 11 columns were erected at the test site, each with a different water-to-cement ratio. Sampling was conducted immediately after column construction, and the samples were stored for analysis over varying curing periods. Fig. 5 illustrates the laboratory and field tests performed on the DSM columns. Finally, the characteristics of the enhanced soil produced by the deep mixing technique were established based on laboratory results, as shown in Table 5.

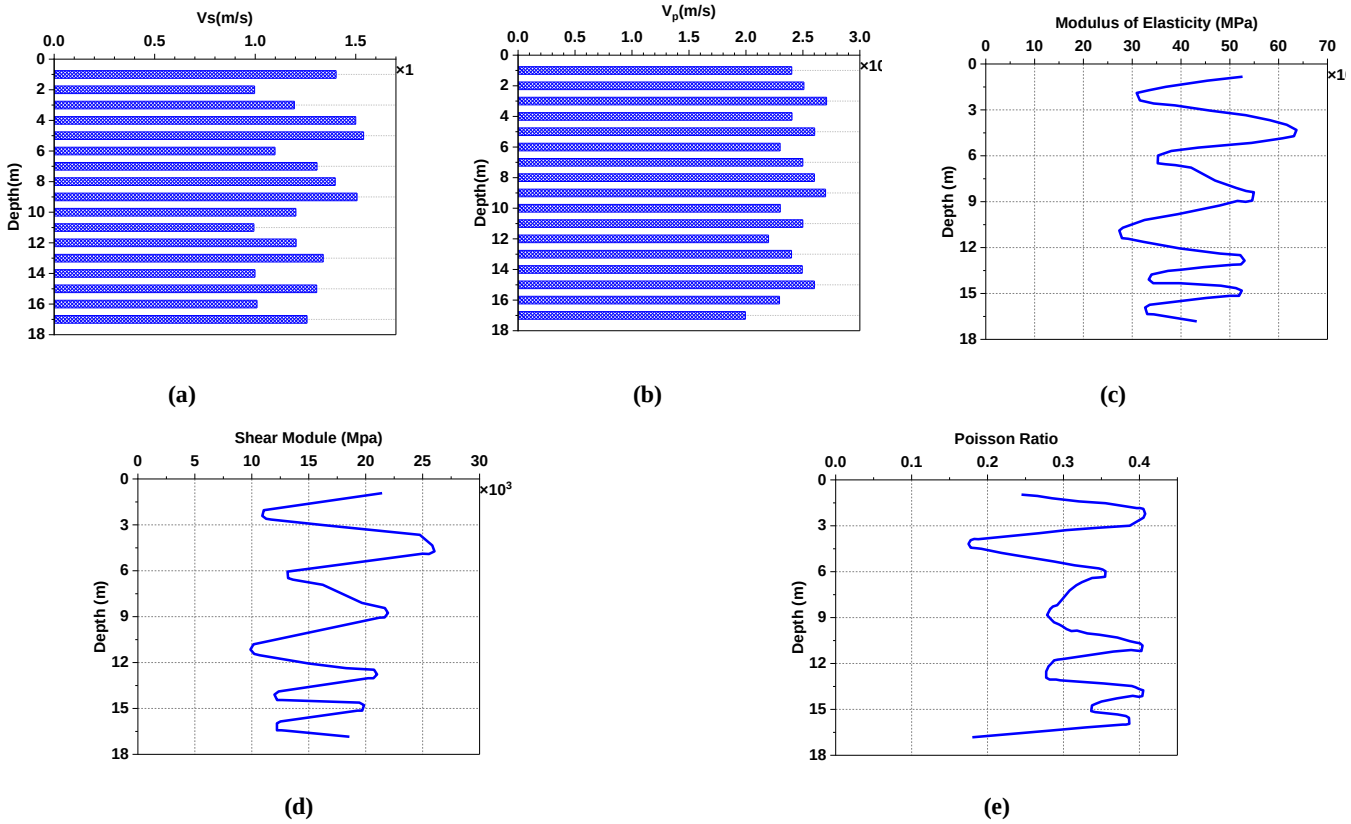


**Fig. 5. Results of laboratory and field tests on DSM.**

**Table 5. Properties of improved soil.**

| Density (t/m$^3$) | S-Wave velocity (m/s) | P-Wave velocity (m/s) |
|---|---|---|
| 2.3 | 1300 | 2400 |

## 3. Numerical modeling

This research examined a two-dimensional linear finite element model addressing soil-structure interaction and structure-soil-structure interaction systems through the open-source software OpenSees version 3.5.0. This tool offers practical resources for analysing structural and geotechnical systems in engineering contexts. GiD version 14.0.1 was employed for both preprocessing and postprocessing. Soil modelling used 4-node quadrilateral elements with a bilinear isoparametric formulation, with elastic and isotropic soil parameters assigned to each element based on laboratory test results. For structural modelling, the elasticBeamColumn element was utilized. An absorbing boundary was established along the lateral and bottom edges of the model using the ASDAbsorbingBoundary2D command, accounting for the soil layer characteristics at each boundary level. To model the interaction between nearby improved and natural soil blocks and between improved soil and the foundation, the degrees of freedom of adjacent nodes were constrained in the vertical and horizontal directions using an equal command. A rigid connection is assumed in the model to accurately reflect the actual behaviour of the substructure–foundation interface. A time-history analysis was performed, using a constant time step and the penalty method to enforce constraint equations. The Krylov-Newton method was selected as the solution algorithm, and convergence was validated using the Norm Displacement Increment Test with a specified tolerance. The RCM numberer, based on the reverse Cuthill-McKee approach, was implemented to link equation numbers with degrees of freedom. The TRBDF2 integrator, a hybrid method combining the trapezoidal rule with the three-point backward-Euler method, was used. In the examined models, a 5% Rayleigh damping was applied to the soil domain, based on laboratory test results and Eqs. 1 and 2.

### *3.1. Mesh size and time step*

The precision of numerical simulations of seismic wave propagation for dynamic soil-structure interaction (SSI) problems is primarily determined by two key parameters: element size and time step. The dimensions of the soil elements (Δh) have been

determined using the Courant-Friedrichs-Lewy (CFL) condition, ensuring that the element size does not exceed one-tenth of the shortest wavelength (λmin). To accurately depict a travelling wave at a specified frequency, at least 10 nodes per wavelength are required. Using fewer than 10 nodes may lead to numerical damping, as the discretization may miss specific peaks in the seismic waves [17, 18].

$$\Delta h \leq \Delta h_{max} = \frac{\lambda_{min}}{10} = \frac{C_{min}}{10 f_{max}} \quad (3)$$

The second stability criterion is linked to the principles of the finite element method. As a wavefront travels through space, it sequentially reaches each node. A sufficiently large time step in the finite element analysis may cause the wavefront to reach two neighbouring nodes simultaneously. This phenomenon contradicts basic wave-propagation theory and may lead to computational instability during simulation. Thus, regulating the time step is crucial for maintaining stability. In this study, the chosen time step ($\Delta t$) was kept smaller than the ratio of the smallest element size to the maximum wave velocity of the soil [18, 19].

$$\Delta t \leq \frac{\Delta h}{C_{max}} \quad (4)$$

Here, $C_{max}$ represents the maximum wave velocity in the soil, and $f_{max}$ represents the maximum earthquake frequency. Based on soil-layer characteristics and the selected earthquake frequency, the element size and time step were determined for each analysis conducted in this study. The input excitation was applied as velocity components at the model's lowest boundary, vertically and simultaneously in both directions.

### *3.2. Boundary condition*

Because the model covers only part of the soil, we must impose artificial boundaries around it. While limiting degrees of freedom at these boundaries is effective for static analyses, it can lead to wave reflections in dynamic analyses. To address this problem, we can position peripheral boundaries sufficiently far from the primary soil area; however, this approach increases analysis time and computational costs. Numerous methods have been suggested for modelling absorbing boundaries. In this study, we adopt Nielsen's method for simulating absorbing boundaries around the soil medium. This method is suitable for two-dimensional and three-dimensional environments, as shown in the two-dimensional diagram in Fig. 5. In this diagram, F represents the free field, which is examined in relation to the primary soil environment; D indicates the Lysmer-Kuhlemeyer dampers that absorb outgoing waves; and T stands for the boundary forces transferred from the free field to the main soil environment via this mechanism [19-21]. In other terms, the lateral boundaries of the main grid are connected to the free-field grid through viscous dashpots to create a quiet boundary (see Figs. 1 to 6). The unbalanced forces from the free-field grid are also exerted on the main grid boundary. Both situations are defined in Eqs. 5 and 6. In which $\rho$ is density; $C_s$, $C_p$ are the p-wave and s-wave speeds at the side boundary; $v_x^m$,$v_y^m$ are the x-velocity and y-velocity of the grid point in the main grid at the side boundary, A is the area of influence of the free-field grid point; $v_x^{ff}$,$v_y^{ff}$ are the x-velocity and y-velocity of the grid point in the side free field; and $F_x^{ff}$,$F_y^{ff}$ are the free-field grid point forces in the x and y directions, respectively [20, 22].

$$F_x = -\rho C_p \left(v_x^m - v_x^{ff}\right) A + F_x^{ff} \quad (3)$$

$$F_y = -\rho C_s \left(v_y^m - v_y^{ff}\right) A + F_y^{ff} \quad (4)$$

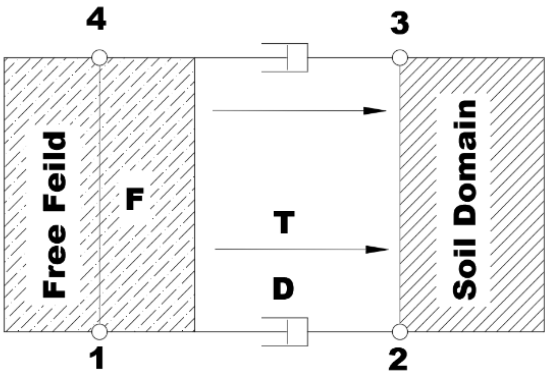


**Fig. 6. A schematic representation of the three key components of an absorbing element [20].**

## 4. Earthquake loading

This study analysed three earthquake acceleration records to assess the effects of earthquake frequency content (refer to Table 6). Beyond soil-structure interaction, the frequency content of earthquake ground motion is crucial in seismic analysis because it significantly affects structural response. To evaluate the frequency characteristics of an earthquake, several indicators are typically used, such as the predominant period, mean period, power spectrum intensity, and the ratio of peak ground acceleration (PGA) in g to peak ground velocity (PGV) in meters per second (m/s) [15, 23, 24]. These parameters provide key insights into the energy distribution and potential damage capacity of seismic waves, particularly regarding the dynamic behaviour of soil and structural systems [14]. The frequency features were evaluated using the Peak Ground Acceleration (PGA)- peak ground velocity (PGV) ratio.

As detailed in Table 6, the earthquakes Northridge-01, Parkfield-02, and Coalinga-03 correspond to low, medium, and high-frequency events, respectively. The records were adjusted to ensure their PGA values reached 0.4g. For the bidirectional earthquake analyses, the vertical acceleration component was estimated to be 2/3 of the horizontal component, yielding a PGA value of 0.27g. Fig. 7 presents the Fourier amplitude spectra and horizontal acceleration response spectra of the scaled earthquake records. In this research, the earthquake velocity records were utilised at a depth of 150 meters within the soil profile.

**Table 6. Properties of earthquake ground motions.**

| Earthquake motion | Station | PGA (g) | PGV (m/s) | PGA/PGV | Frequency content | Predominant period (sec) | | Type |
|---|---|---|---|---|---|---|---|---|
| | | | | | | Horizontal component | Vertical component | |
| **Northridge-01** | Pardeee | 0.55 | 0.76 | 0.723 | Low | 0.75 | 0.12 | Pulse |
| **Parkfield-02, CA** | Parkfield - Cholame 1E | 0.23 | 0.44 | 1.1 | Intermediate | 0.16 | 0.14 | Pulse |
| **Coalinga-03** | Burnett Construction | 0.167 | 0.07 | 2.38 | Hight | 0.2 | 0.14 | No Pulse |

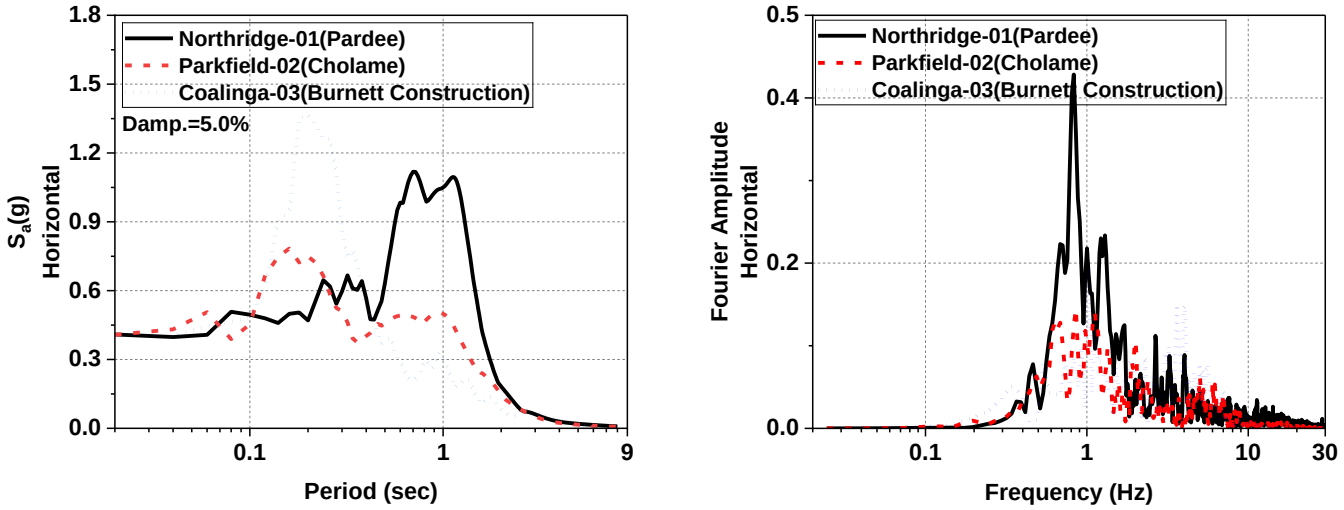


(a) (b)

**Fig. 7. Acceleration response spectra and Fourier amplitude spectra of the earthquake records scaled to the target PGA and used in the analyses.**

In this study, earthquake records were selected primarily based on the PGA/PGV ratio, a widely accepted indicator for distinguishing the frequency content of ground motions, enabling comparison of pulse-like records with dominant low-frequency content and records characterized by higher-frequency components [15]. The primary objective was to investigate the sensitivity of the seismic response of the soil–DSM–foundation–structure system to general variations in input frequency content, rather than to perform an entirely site-specific near-fault calibration. Ground-motion parameters such as the directivity pulse period (TP), significant duration, and vertical-to-horizontal spectral ratios (V/H) are recognized as essential factors in advanced near-fault seismic analyses, particularly in nonlinear response assessments and site-specific design frameworks. However, the simultaneous consideration of these parameters requires a comprehensive site-specific approach based on probabilistic seismic hazard analysis (PSHA) and the selection of ground motions compatible with both vertical and horizontal target spectra. Such an approach was beyond the scope of the present study. The focus of this research is on identifying the dominant physical mechanisms governing vertical acceleration amplification, including foundation rocking, structure–soil–structure interaction (SSSI), and the influence of block-type deep soil mixing (DSM). The results indicate that the observed amplification patterns are primarily driven by these interaction mechanisms rather than by the specific characteristics of individual near-fault records. Consequently, although parameters such as TP or V/H may affect the absolute magnitude of the responses, they are not expected to alter the qualitative trends or the governing mechanisms identified in this study. Future studies may extend this work by incorporating advanced near-fault ground-motion parameters, including frequency-dependent *V/H* ratios and more realistic soil stratification conditions (e.g., nonparallel soil layers), within an entirely site-specific seismic assessment framework [25].

## 5. Verification

### *5.1. Benchmark 1*

An examination of the elastic phase model proposed by Uzun and Ayvaz [26] was conducted to evaluate the validity of the models developed in this study. As shown in Fig. 8a, an elastic soil model was constructed according to the specifications outlined in Table 7, with the PDML boundary defined around the soil layer to assess the performance of the absorbing boundaries. As illustrated in Fig. 8b, a Ricker wave load, characterized by an amplitude of 100 kN, a frequency of $f$ = 5 Hz, and a duration of $t$ = 3 sec, was applied at point P1. The resulting displacements, obtained from both the study and the analyses performed in this work, are presented in Fig. 9.

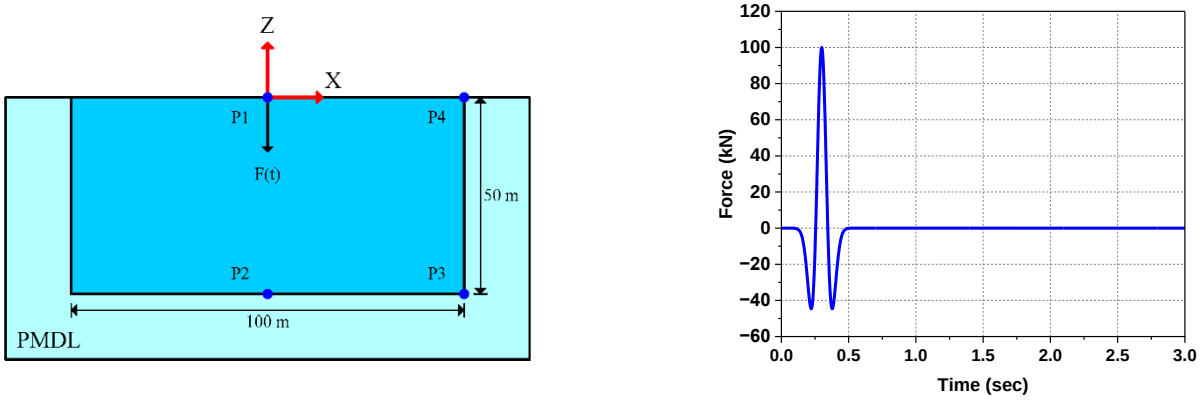


**(a)** **(b)**

**Fig. 8. (a) The PDML truncated domain [26], (b) Input force history [26].**

**Table 7. Model properties [26].**

| Density (t/m³) | S-Wave velocity (m/s) | Poisson | m | n |
|---|---|---|---|---|
| 2 | 400 | 0.3 | 9 | 2 |

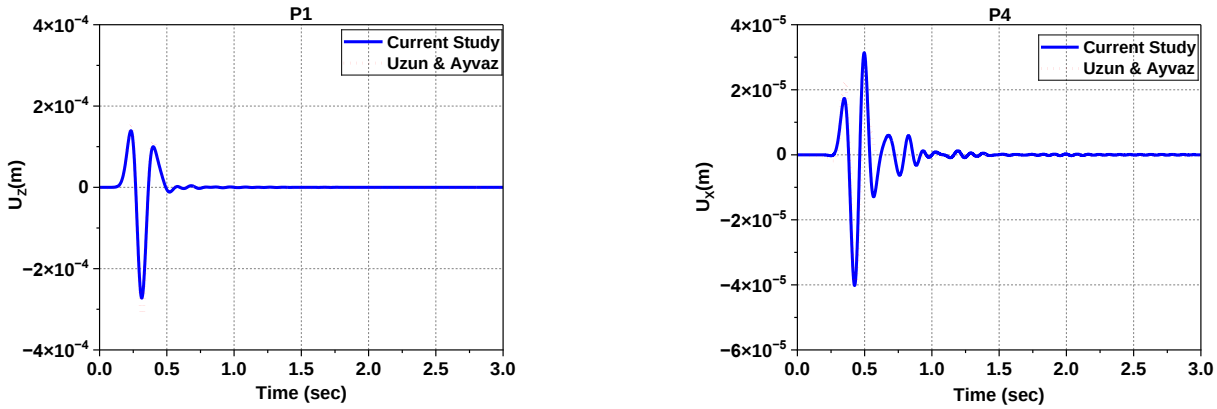


**(a)** **(b)**

**Fig. 9. (a) vertical displacement at P1; (b) horizontal displacement at P4 [26].**

*5.2. Benchmark 2*

To verify the accuracy of the elastic-phase modeling, the behavior of a single soil layer was examined in both two-dimensional (2D) and three-dimensional (3D) configurations (Fig. 10). In both models, lateral and bottom boundaries were simulated using a combination of free-field columns and Lysmer–Kuhlemeyer semi-infinite elements to prevent wave reflections. The mechanical properties of the soil layer were taken from Table 8.

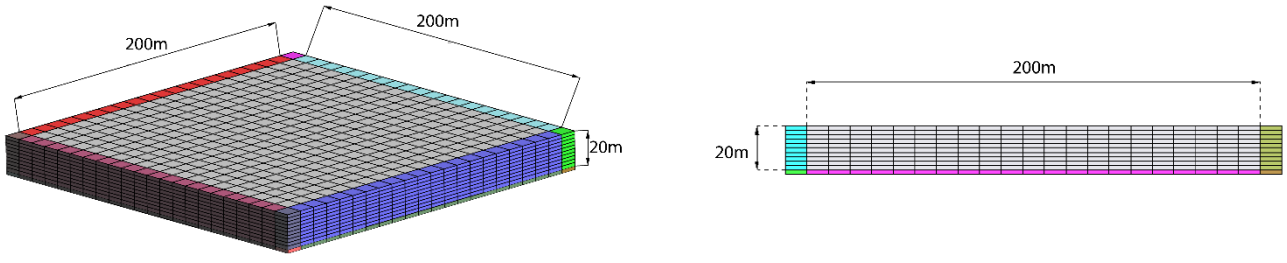


**(a)** **(b)**

**Fig. 10. Two-dimensional and three-dimensional soil layer models with dimensions of (a) 200 × 200 × 20 m³, (b) 200 × 20 m².**

**Table 8. Properties of the single-layer soil.**

| Material | Modulus of elasticity (kPa) | Density (t/m³) | Poisson ratio |
|---|---|---|---|
| Soil | $100 \times 10^6$ | 2 | 0.3 |

The models were subjected to Ricker-wave excitation with a peak acceleration of 1g and a frequency of 4 Hz. According to

theory, for a semi-infinite, elastic, undamped, single-layer soil medium under a wave with peak acceleration A, the maximum acceleration at the ground surface is expected to reach 2A due to the superposition of incident and reflected waves [27]. As shown in Fig. 11, the ground surface acceleration reaches a peak of $B$ = 2g, the input acceleration at the base is $A$ = 1g, and the reflected wave at the surface is $C$ = 1g, confirming that the incident and reflected wave amplitudes are equal ($A$ = $C$) and resulting in the expected doubling at the surface. Furthermore, the results demonstrate strong agreement between the 2D and 3D models, confirming the reliability and validity of the numerical model in the elastic phase.

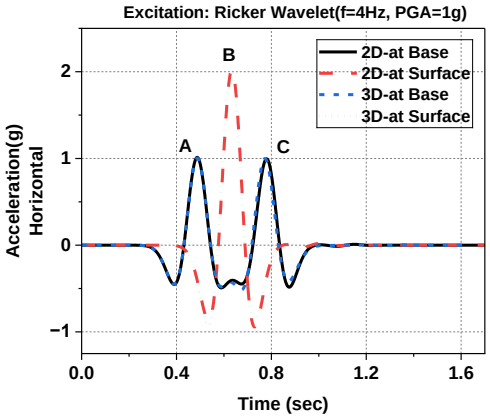


**Fig.11. Recorded acceleration time histories at the base and ground surface for a single-layer elastic soil under a Ricker wavelet excitation ($f$ = 4 Hz, PGA = 1 g) in 2D and 3D models.**

## 6. Impact of soil domain size on seismic response: sensitivity study

One of the key factors affecting the accuracy of seismic analyses is the selection of an appropriate soil domain size relative to the foundation dimensions. For instance, ASCE/SEI 4-16: Seismic Analysis of Safety-Related Nuclear Structures states that viscous dashpots, installed normal and tangential to the lateral boundaries, should be located at a minimum distance of four to five foundation radii from the edge of the structure. These boundaries are not perfectly absorbing, and their effectiveness is reduced by wave scattering at oblique incidence. The code recommendation applies when model boundaries are simulated using only Lysmer–Kuhlemeyer dashpots. In this study, as detailed in Section 2-3 and schematically shown in Figs. 1 and 6, a combination of free-field soil columns and Lysmer–Kuhlemeyer dashpots was used along the lateral and bottom boundaries to provide a more effective absorbing boundary. Furthermore, a sensitivity analysis with varying model dimensions was conducted: soil domains of 400 m × 150 m and 200 m × 120 m were analyzed under unidirectional Coalinga-03 earthquake loading, and DSM blocks were modeled with a width of 50 m, a thickness of 8 m, and a foundation thickness of 3 m. The results, shown in Fig. 12, indicate complete agreement in the seismic response of the improved soil, and the effects of boundary reflections or wave interference on the rocking-induced vertical response were negligible.

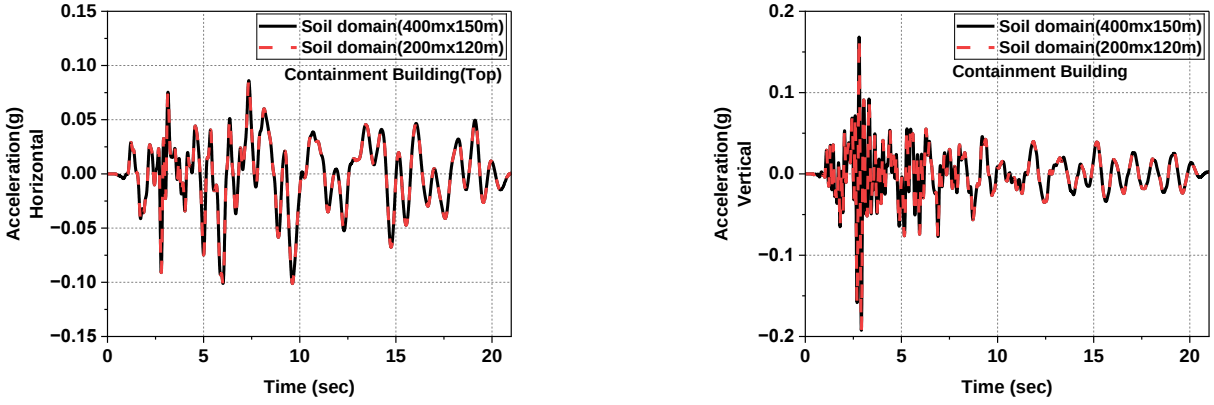


**Fig. 12. Consistency of Containment Building Response across different model dimensions.**

## 7. Result

### *7.1. The effect of a unidirectional loading*

In this section, the effects of modeling the DSM layer with thicknesses of 8 m and 18 m beneath the 3-m-thick foundation slab on the seismic response of the containment building and the internal structure are investigated. The soil–structure interaction response of the reactor system is evaluated under unidirectional seismic excitation, in which the input motion is applied in the x-direction and propagates in the y-direction. Fig. 13 presents the horizontal and vertical accelerations induced by rocking motion, along with their Fourier amplitude spectra, at the top levels of the containment building ($x$ = 78 m) and the internal structure ($x$ = 34.5 m). Although both the Parkfield and Coalinga ground motions were recorded in the near-fault region, they exhibit distinct

frequency characteristics. The results indicate that, in all cases, the internal structure experiences higher horizontal accelerations compared with the containment building. Moreover, due to the reactor system's large mass and geometric dimensions, and the significant stiffness contrast between the block-type DSM improvement layer and the surrounding natural soil, vertical accelerations associated with rocking motion are observed in all numerical models. Because the lumped mass representing the containment building is located farther from the center of the foundation and the DSM region, the resulting vertical acceleration in this structure is consistently larger than that in the internal structure. For the Parkfield earthquake, the DSM layer has negligible influence on the horizontal acceleration amplitude at frequencies above 1 Hz in the containment building. At lower frequencies, however, the response becomes more sensitive; below 0.5 Hz, the 18-m-thick DSM layer produces the largest increase in horizontal acceleration, whereas in the 0.5–1 Hz range the DSM layer reduces the acceleration amplitude. The internal structure shows lower sensitivity to DSM improvement; however, at 0.5 Hz, the DSM layer increases the horizontal acceleration, with DSM thicknesses of 8 m and 18 m amplifying the response by approximately 25% and 35%, respectively. A similar pattern is observed for the Coalinga earthquake at higher frequencies, where the DSM layer does not affect the horizontal acceleration amplitude of either structure above 1 Hz. In the low-frequency range of 0.1–0.6 Hz, the presence of DSM increases the horizontal acceleration of the containment building. Conversely, in the 0.6–1 Hz band, the DSM layer reduces horizontal acceleration; thicknesses of 8 m and 18 m reduce the amplitude by approximately 31% and 47%, respectively. Within the internal structure, the DSM layer again shows no significant influence above 1 Hz; however, at frequencies below 0.5 Hz, it reduces horizontal acceleration by approximately 24% for the 8-m layer and 26% for the 18-m layer. As observed for the Parkfield motion, amplification occurs at around 0.5 Hz when DSM is present. The effect of DSM on the vertical acceleration associated with rocking motion is not uniform at frequencies below 2 Hz in either earthquake. Depending on the frequency, the DSM layer may amplify or attenuate vertical acceleration. Nevertheless, a consistent and prominent trend is observed across both structures and seismic motions: in the 2–10 Hz frequency range, the DSM layer and its thickness significantly amplify vertical acceleration. For the Parkfield earthquake, the 18-m-thick DSM layer increases the vertical acceleration by 147% in the containment building and by 59% in the internal structure. Under the Coalinga motion, the same DSM thickness results in increases of 141% and 58% in the containment building and internal structure, respectively. Given that many reactor-building components have natural frequencies within this range and are highly sensitive to vertical acceleration, evaluating the impact of block-type DSM improvements on the seismic performance of high-frequency equipment in nuclear facilities is critical.

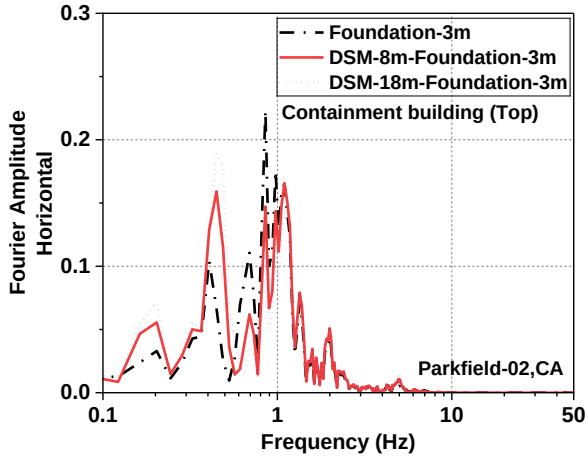


(a)

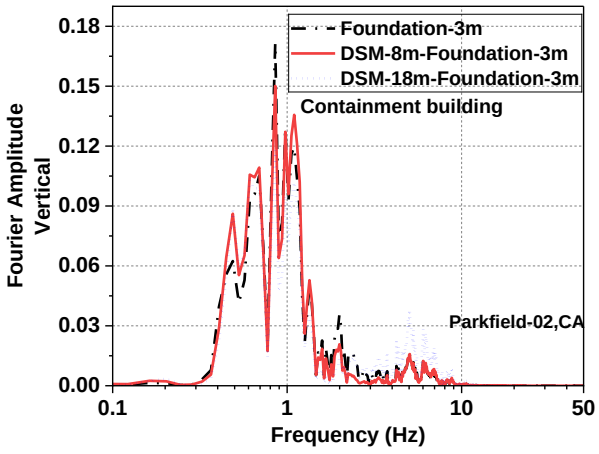


(b)

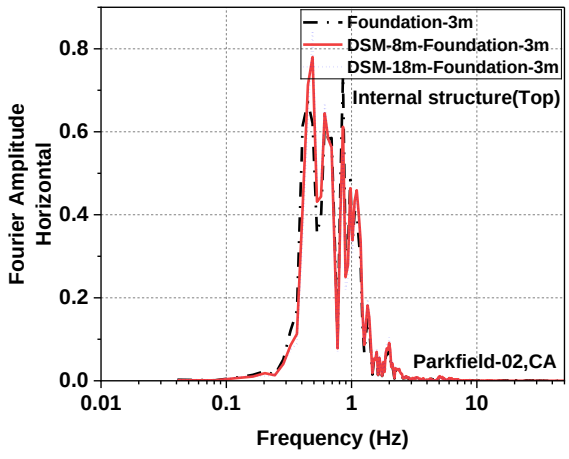


(c)

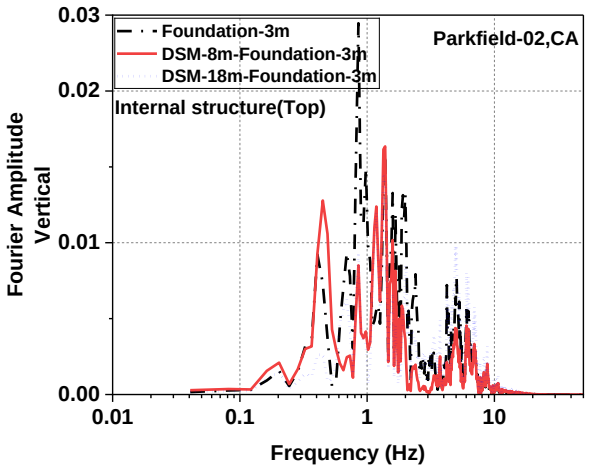


(d)

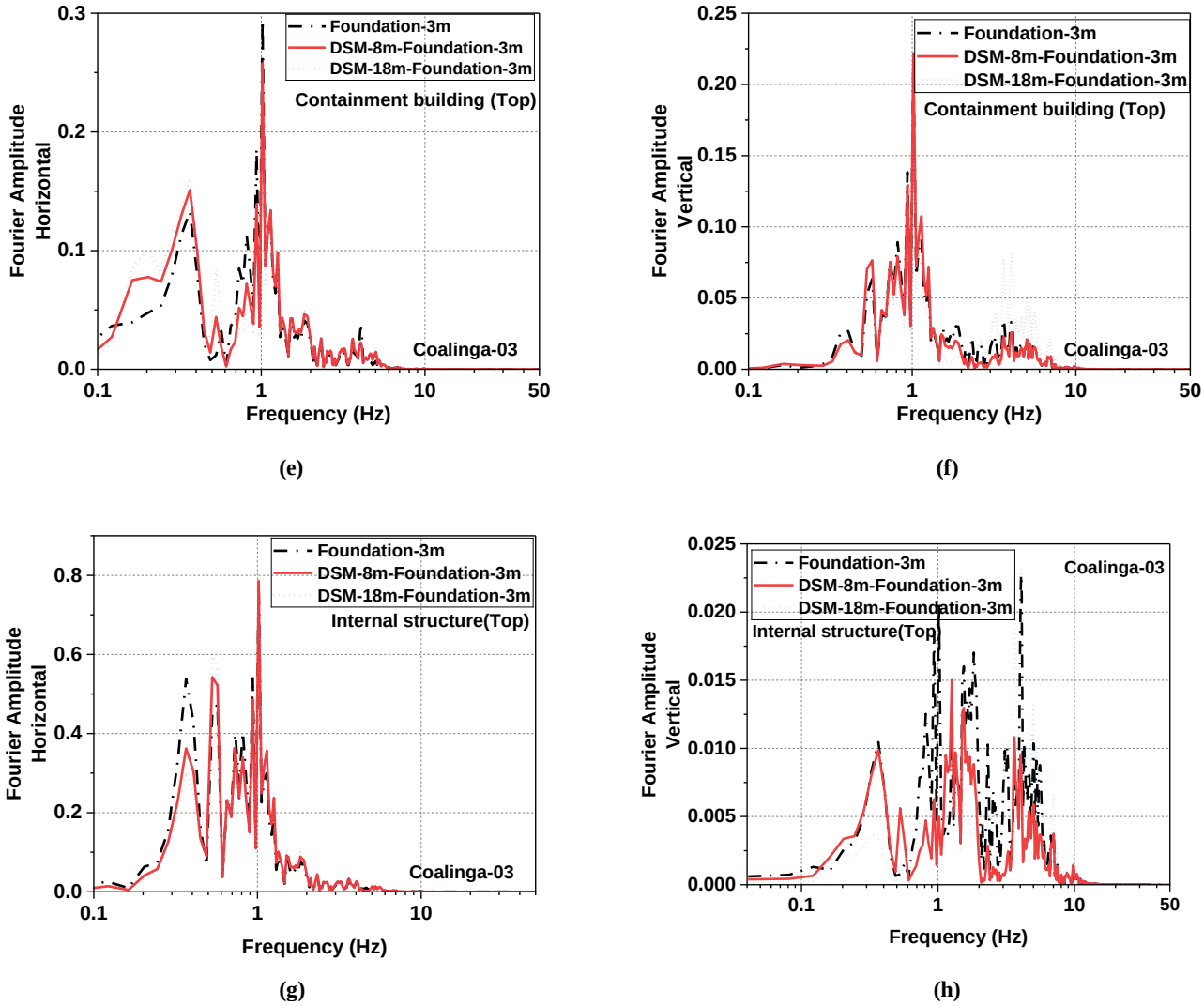


**Fig. 13. Fourier amplitude spectra of horizontal and vertical accelerations for the internal structure and the containment building under unidirectional seismic excitation: (a–d) Parkfield-02CA; (e–h) Coalinga-03.**

As noted in the literature and regulatory guidelines, for soft soils (Site Class D–F) or when shear strains exceed approximately 0.5%, nonlinear analyses are generally required to properly account for strain-dependent modulus degradation (G/Gmax) and increased hysteretic damping [17]. However, the primary objective of this study was to identify the dominant physical mechanisms governing vertical-acceleration amplification, particularly foundation rocking and soil–structure–structure interaction (SSSI), in the presence of block-type deep soil mixing (Block-Type DSM). Accordingly, a linear-elastic modeling approach was adopted as a conservative and transparent framework for interpreting these mechanisms. In previous studies conducted on Nevada sand, assuming elastoplastic soil behavior and block-type DSM improvement, it was observed that vertical accelerations induced by foundation rocking under unidirectional loading primarily occur within the dominant frequency range of nuclear power plant structures. Under bidirectional loading, however, vertical acceleration amplification was observed across a broader frequency range [28]. These findings indicate that even when soil nonlinearity is accounted for, the overall pattern of vertical-acceleration amplification and the governing mechanisms, particularly foundation rocking and SSI/SSSI effects, remain essentially unchanged. Furthermore, nonlinear soil modeling is expected to have a greater influence on horizontal responses of nuclear structures. Therefore, the observed amplification of vertical accelerations in the 2–10 Hz frequency range should not be attributed solely to the linear soil assumption; instead, it originates from the interactive mechanisms of the soil–DSM–foundation–structure system. To analyze the time–frequency distribution of energy, both the Continuous Wavelet Transform (CWT) with the Morlet wavelet and the S-Transform (ST) can be applied. A comparison of the two methods shows that CWT with Morlet wavelet captures transient energy bursts and short-term concentrations more accurately, which is particularly useful for identifying dominant vibration modes and energy focus in short time intervals. In contrast, S-Transform provides a broader frequency representation with fixed time resolution, suitable for overall spectral analysis, but it is less precise in localizing transient energy [29, 30]. Considering the objective of this study, to identify energy concentrations and dominant modes of the soil–structure system in short time windows, the Morlet wavelet transform was selected as the primary method. At the same time, the S-Transform can serve as a complementary tool for general spectral analysis. Fig. 14 presents the Morlet wavelet power spectrum of vertical accelerations induced by rocking motion and horizontal accelerations in the containment building under unidirectional excitation of the Coalinga earthquake. As shown in Fig. 14a and 14b, the presence of the DSM layer reduces the energy of horizontal acceleration transmitted to the containment building while simultaneously concentrating it within the higher-frequency range. Fig. 14d indicates that the 18-m-thick block deep-mixing (BDM) layer increases

the vertical-acceleration energy applied to the containment building. The vertical-acceleration energy is particularly concentrated around 3 seconds and in the frequency range 3–7 Hz. This high-frequency energy concentration, resulting from the block deep-mixing modeling, may significantly affect the seismic performance of nuclear power plant structures and sensitive equipment and should therefore be carefully considered in the design.

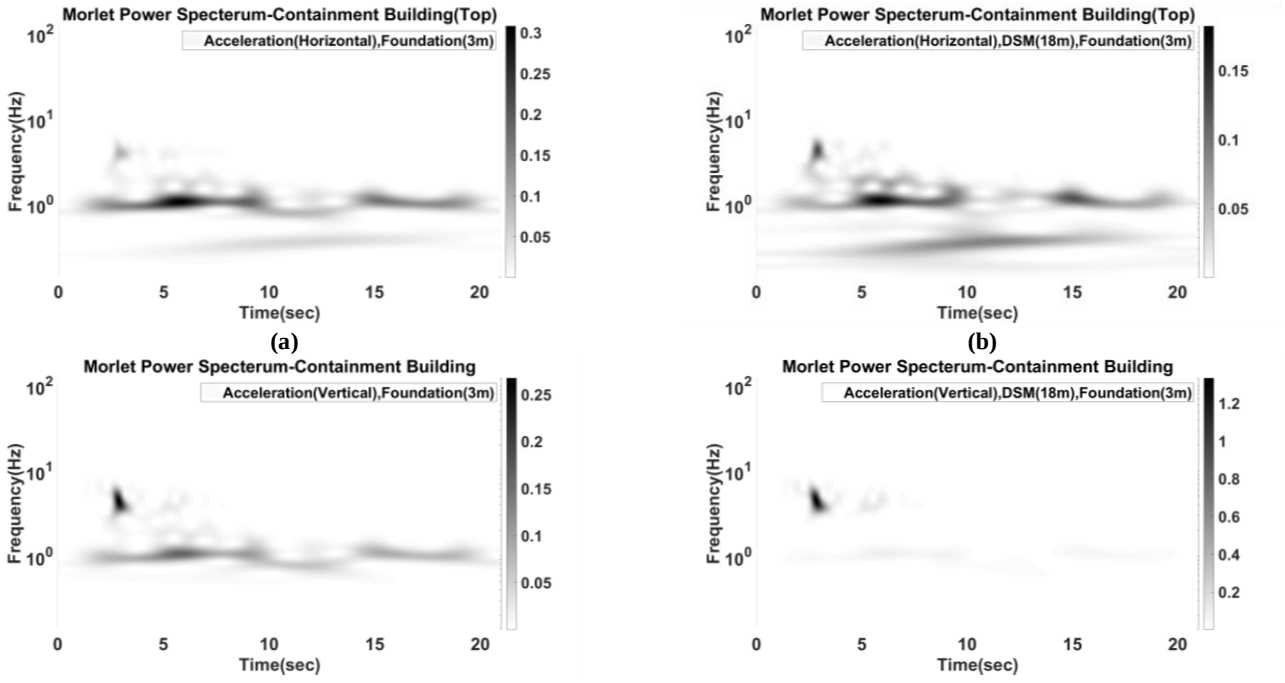


**Fig. 14. Morlet wavelet power spectrum of vertical accelerations induced by rocking motion and horizontal accelerations in the containment building under unidirectional excitation of the Coalinga earthquake.**

The substantial amplification of vertical accelerations observed in the presence of DSM layers may result from multiple physical mechanisms. In this study, the focus was primarily on evaluating the relative contribution of foundation rocking-induced soil–structure interaction (SSI) and the effect of DSM itself. Our results indicate that the effectiveness of block-type deep soil mixing in mitigating horizontal accelerations becomes significant only when there is a considerable dynamic impedance contrast between the DSM-improved soil and the surrounding natural soil. Yaghfoori et al. [14, 28] showed that the influence of this impedance contrast on horizontal and rocking-induced vertical accelerations was systematically investigated. This study included a parametric assessment of DSM stiffness, based on laboratory results from the ongoing nuclear power plant project, considering variations in the water-to-cement ratio of the DSM grout (ranging from 1.7 to 3). The findings demonstrated that achieving acceptable DSM performance in controlling horizontal accelerations requires a substantial stiffness difference between the improved zone and the surrounding soil. Furthermore, variations in the water-to-cement ratio within the tested range had minimal impact on vertical accelerations induced by foundation rocking. This indicates that rocking motion is the dominant mechanism driving vertical-acceleration amplification, whereas the impedance contrast primarily facilitates its occurrence. The reduction of horizontal accelerations recorded at the ground surface in the vicinity of zones improved by the block-type deep soil mixing (DSM) method can be primarily attributed to the substantial increase in stiffness and dynamic impedance of the treated soil relative to the surrounding natural ground. This impedance contrast leads to partial reflection, scattering, and redirection of seismic waves with dominant horizontal components at the boundaries of the DSM block, thereby limiting the effective transmission of horizontal ground motion to the surface in the near-field region of the improved zone. Moreover, the presence of a stiff, relatively massive DSM block alters the kinematic soil–structure interaction mechanism, thereby intensifying the coupling between translational and rocking motions of the foundation. As a result, a portion of the incoming horizontal seismic energy is redistributed from translational modes into rotational (rocking) modes, which may, in turn, increase vertical accelerations associated with rocking behavior. This redistribution of seismic energy plays a significant role in reducing the amplitude of horizontal ground surface accelerations in the vicinity of the DSM block. In addition, the DSM block may act as a frequency-dependent filter, particularly attenuating the higher-frequency components of the input ground motion. This filtering effect is directly related to increased stiffness and modified wave-propagation conditions within the improved soil mass. Furthermore, it reduces horizontal accelerations near the treated area. It should be emphasized that this reduction in horizontal acceleration is inherently spatial and distance-dependent. At locations farther from the DSM block, phenomena such as wave diffraction, refraction, and re-concentration of seismic energy may amplify horizontal accelerations. This observation indicates that the influence of block-type deep soil mixing on the seismic response of the ground surface and adjacent structures is strongly dependent on the geometry of the DSM block, the spacing between structures, the soil's dynamic properties, and the frequency content of the input earthquake motion. Consequently, a general conclusion cannot be drawn; case-specific, project-oriented evaluations are required. Accordingly, it can be concluded that block-type deep soil mixing should not be regarded merely as a soil improvement technique, but rather as a modification to the seismic wave propagation path, whose effects on horizontal ground surface accelerations are governed by dynamic impedance contrast, wave scattering mechanisms, and rocking-induced soil–structure interaction phenomena.

### *7.2. The effect of a bidirectional loading*

Near-fault earthquakes, characterized by distinct dynamic features such as velocity pulses and high-frequency content, can significantly affect the seismic response of structures [12, 31]. A notable characteristic of these motions is the strong high-frequency vertical component, which may in some cases exceed the horizontal component. This phenomenon is particularly critical for nuclear reactor buildings, where internal equipment typically has high natural frequencies and is highly sensitive to vertical accelerations. Mechanical and electrical systems, as well as piping networks, are therefore highly vulnerable to damage or malfunction caused by vertical vibration. The presence of a strong vertical component can also increase axial forces in columns, reduce connection capacities, and promote brittle failure mechanisms. Consequently, the seismic design of nuclear facilities in high-hazard, near-fault regions requires careful consideration of vertical excitation effects, detailed frequency-domain analyses, and realistic soil–structure interaction modeling. In this study, the seismic behavior of the APR1400 reactor structure (Fig. 1) is evaluated under bidirectional near-fault ground motions, including the Northridge earthquake recorded at the Pardee station and the Coalinga earthquake (Table 6). As previously noted, the horizontal component is scaled to 0.4g and the vertical component to two-thirds of that value (0.27g). In the analytical models developed in this section, the reactor structure is modeled on a 3-m-thick foundation slab underlain by an 18-m-thick block deep-mixing (BDM) improvement layer. Fig. 15 presents the Fourier amplitude spectra of horizontal and vertical accelerations in both the containment building and internal structure under unidirectional and bidirectional loading. The results show that bidirectional loading has little influence on horizontal acceleration but substantially amplifies vertical acceleration. For the Northridge record, vertical components above 1 Hz show average amplification factors of 17 (containment building) and 46 (internal structure). For the Coalinga record, vertical components between 0.1 and 10 Hz increase by factors of 6 and 25, respectively. Given that many nuclear plant components have natural frequencies within this range, evaluating seismic response under two- and three-directional excitations is essential, particularly in near-fault regions.

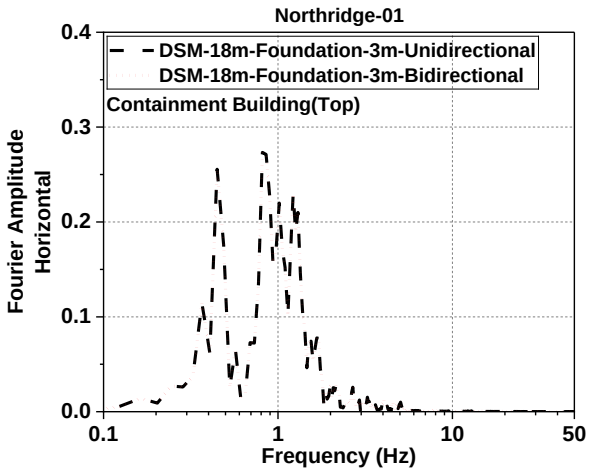


(a)

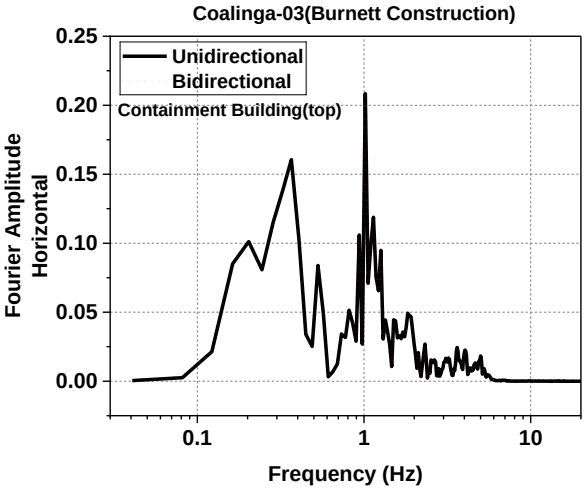


(e)

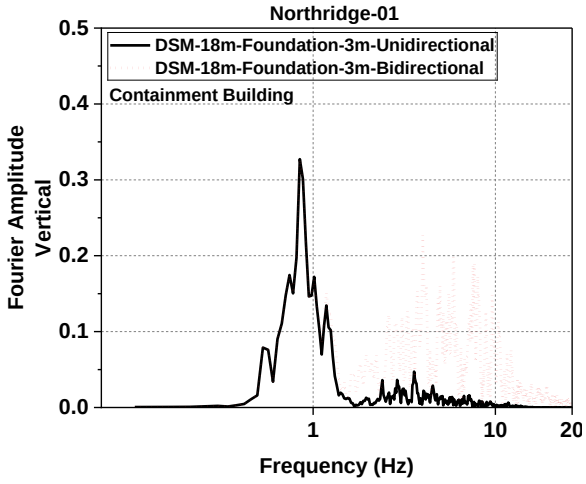


(b)

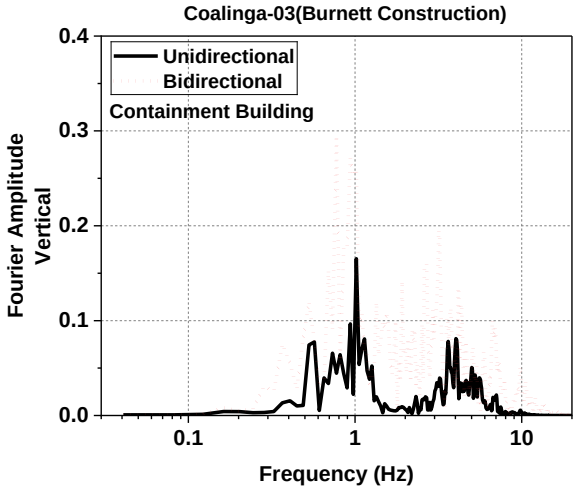


(f)

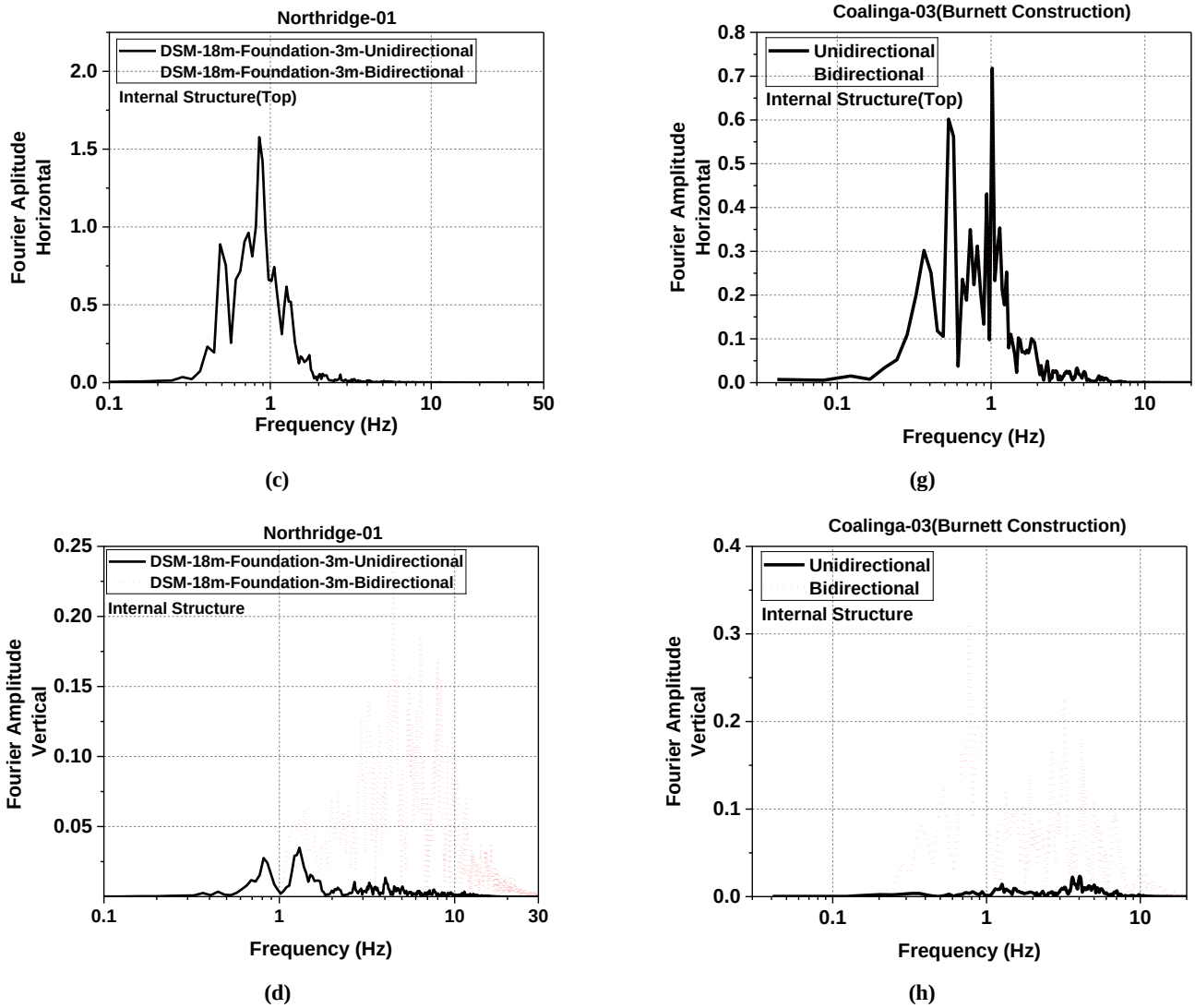


**Fig. 15. Fourier amplitude spectra of horizontal and vertical accelerations for the containment building and the internal structure under unidirectional and bidirectional seismic excitations.**

Fig. 16 presents the Fourier amplitude spectra of horizontal and vertical accelerations in the containment building and the internal structure under bidirectional excitation of the high-frequency Coalinga earthquake. As shown in Fig. 16a, the difference in horizontal acceleration at the upper levels of the two structures is significant. For frequencies below 0.3 Hz, the horizontal acceleration amplitude in the containment building is, on average, 45% higher than that of the internal structure. However, within the frequency range of 0.3–4 Hz, the average horizontal acceleration amplitude of the containment building is 196% lower than that of the internal structure. For frequencies above 4 Hz, the acceleration amplitudes in both structures are nearly equal. These variations in horizontal acceleration response may affect the performance of connections between the internal structure and the containment building and should therefore be considered in the design. The Fourier amplitude spectra of vertical acceleration in Fig. 16b show that the differences in vertical acceleration between the two structures are smaller than those in the horizontal component. In specific frequency ranges, the internal structure exhibits higher vertical acceleration amplitudes, whereas in other ranges the containment building exhibits larger vertical acceleration amplitudes.

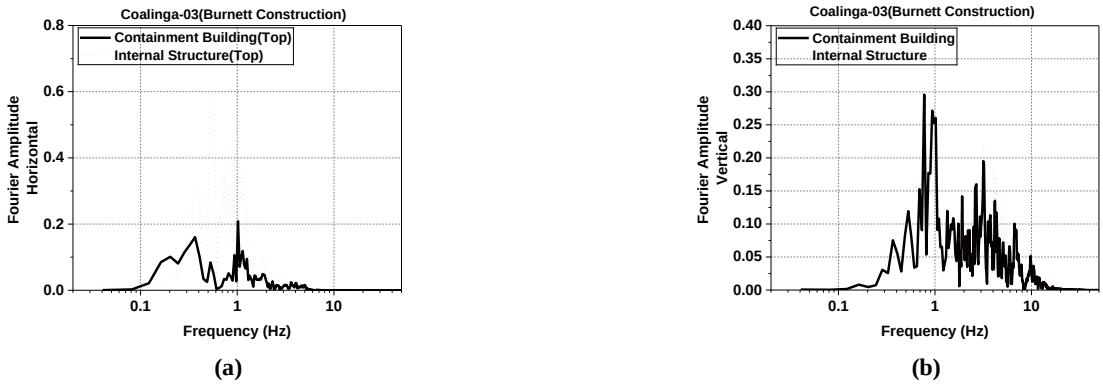


**Fig. 16. Fourier amplitude spectra of horizontal and vertical accelerations in the containment building and the internal structure under bidirectional excitation of the Coalinga earthquake.**

Fig. 17 presents the Morlet wavelet power spectrum of horizontal and vertical accelerations in the containment building under unidirectional and bidirectional excitation of the Coalinga earthquake. As observed, bidirectional loading does not significantly affect the energy of horizontal acceleration transmitted to the containment building. Still, it increases the energy of vertical acceleration and concentrates it at higher frequencies. This high-frequency energy concentration likely results from the combined effects of multiple-directional motion and the complex interaction between the structure and the DSM improvement layer. The amplification of vertical acceleration, particularly at higher frequencies, may significantly influence the seismic performance of the structure and sensitive equipment within the containment building, and should be carefully considered in seismic design and safety assessments.

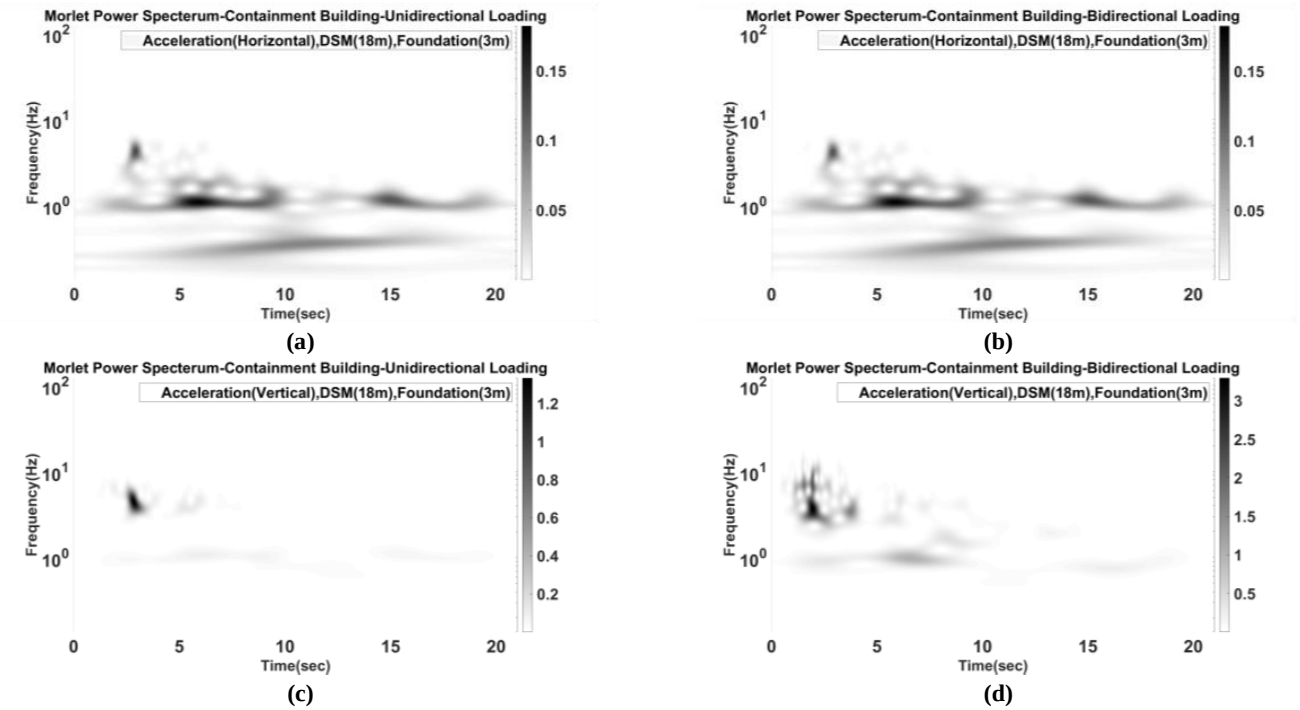


**Fig. 17. Morlet wavelet power spectrum of horizontal and vertical accelerations in the containment building under unidirectional and bidirectional excitation of the Coalinga earthquake.**

Clause C2.5.3 of ASCE 4-16 (Seismic Analysis of Safety-Related Nuclear Structures) states that the vertical-to-horizontal acceleration ratio (V/H) depends on earthquake frequency, source-to-site distance, local soil conditions, and, to a lesser extent, earthquake magnitude and faulting style. This ratio is typically determined through a site-specific probabilistic seismic hazard analysis (PSHA). If PSHA does not provide a V/H value, the analyst should select an appropriate and well-justified value. For near-fault sites (within 15 km), Holocene soils, or locations with thick soil layers, the V/H ratio should be explicitly calculated. For all other conditions, a conservative value of 2/3 is recommended for all frequencies. Studies by Bozorgnia and Campbell [32] have shown that the natural period, local soil conditions, and source-to-site distance strongly influence the V/H ratio. At the same time, its dependence on earthquake magnitude, faulting mechanism, and sediment depth is weaker. Near the fault, this ratio can reach 1.8 for short periods. However, for near-fault regions, code-specified values require a site-specific PSHA; for other conditions, a value of 2/3 is considered conservative and appropriate. Considering that the primary objective of this study was to assess the overall seismic behavior of the APR1400 reactor on DSM-improved soil, the simplified assumption of the minimum value recommended by ASCE 4-16, i.e., a vertical-to-horizontal acceleration ratio of 2/3, was adopted as the basis for the analyses. The results of Tyapin's [33] study indicate that the weight of the DSM-improved soil blocks and structure is only one of the factors influencing vertical accelerations under bidirectional loading, and its effect is negligible. Given the high-frequency content of the vertical component of ground motion, vertical accelerations are transmitted directly to the ground surface with minimal attenuation. In this study, by assuming elastic behavior for both soil and structure, this direct transmission of vertical accelerations has been confirmed. Therefore, even if the vertical-to-horizontal acceleration ratio exceeds 2/3, the overall pattern of vertical acceleration amplification and the dominant mechanism (foundation rocking and SSSI) remain unchanged, although the numerical values of vertical accelerations increase proportionally with the input ratio.

### *7.3. The effect of Structure -Soil-Structure interaction*

In densely built-up areas, such as power plant islands where reactors, turbines, and other vital facilities are located in close proximity, vibrations from one structure can induce secondary motions in nearby buildings. This can lead to operational issues or even structural damage. This section evaluates the seismic response of the two adjacent structures of the APR1400 reactor, which were modeled simultaneously in the numerical analysis. To assess the effects of structure–soil–structure interaction (SSSI), as shown in Fig. 18, two APR1400 reactor buildings, spaced 30 m and 70 m apart, were modeled on a shared soil medium and subjected to horizontal ground shaking using the Northridge-01 near-fault earthquake record (see Table 6).

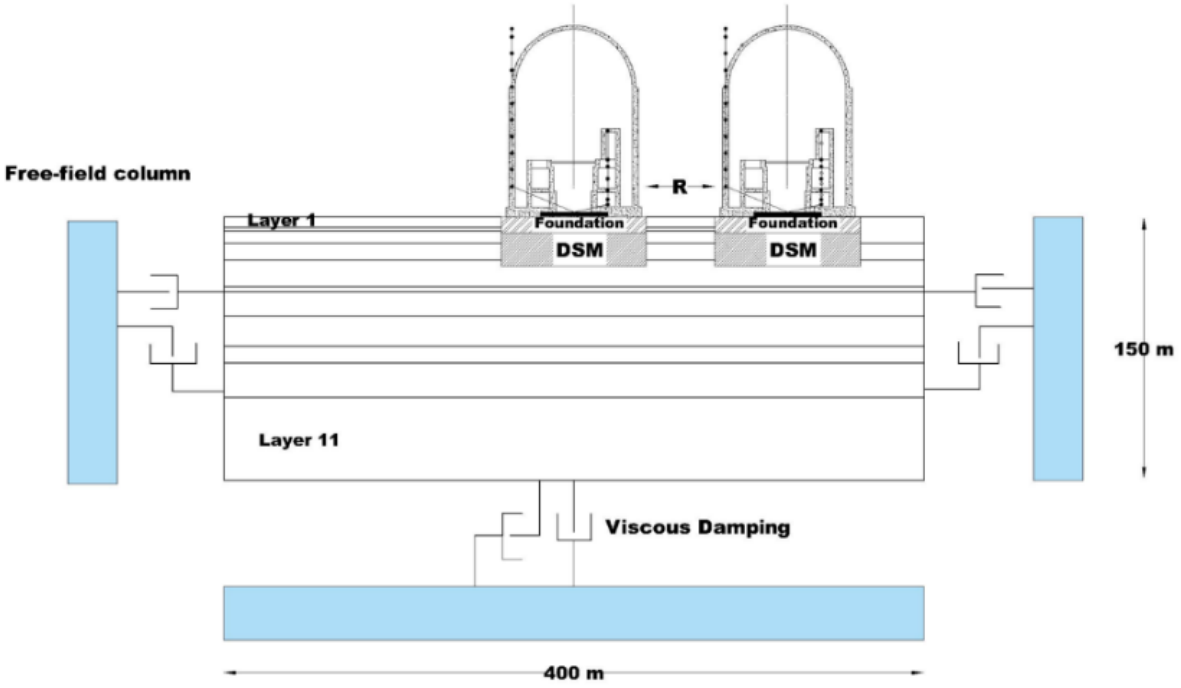


**Fig. 18. SSSI models of the reactor pairs separated by distance R.**

Fig. 19 illustrates the Fourier amplitude spectra of the horizontal acceleration at the upper levels of the internal structure and the containment building, as well as the vertical acceleration induced by rocking motion, under the unidirectional excitation of the Coalinga earthquake while accounting for structure–soil–structure interaction (SSSI). The results indicate that the influence of SSSI on the vertical acceleration component is considerably more pronounced than on the horizontal component in both structures. For the horizontal component, the presence of the adjacent structure results in only a slight reduction in acceleration amplitude, which is more pronounced for the second-reactor model at 30 m. For the containment building, SSSI reduces the vertical-acceleration amplitude at frequencies below 1.5 Hz, with average reductions of approximately 52% and 30% for the second-reactor model at separation distances of 30 m and 70 m, respectively. However, in the 1.5–10 Hz frequency range, SSSI increases vertical acceleration, with amplification of about 39% at 30 m and 5% at 70 m. In the internal structure, SSSI consistently amplifies the vertical acceleration across all frequencies. At frequencies below 1.5 Hz, the largest vertical acceleration occurs for the second-reactor model at 30 m, whereas in the 1.5–10 Hz range, the maximum amplitudes correspond to 70 m. This behavior suggests that the effect of SSSI is strongly dependent on both the separation distance between the structures and the frequency content of the input motion, resulting in distinct patterns of amplification or attenuation. Overall, the findings show that SSSI predominantly amplifies the vertical acceleration in the higher-frequency range. This is particularly critical for nuclear power plant facilities, as many safety-related components and equipment possess high natural frequencies and are highly sensitive to vertical excitation. Neglecting SSSI may therefore lead to an underestimation of vertical acceleration demands, potentially compromising the seismic safety of high-frequency systems. Consequently, accurate assessment of SSSI effects is essential in the seismic design of closely spaced structures within the nuclear power plant island.

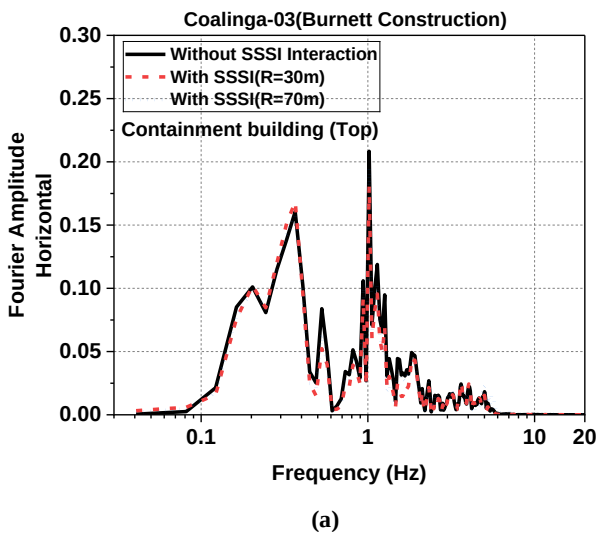


(a)

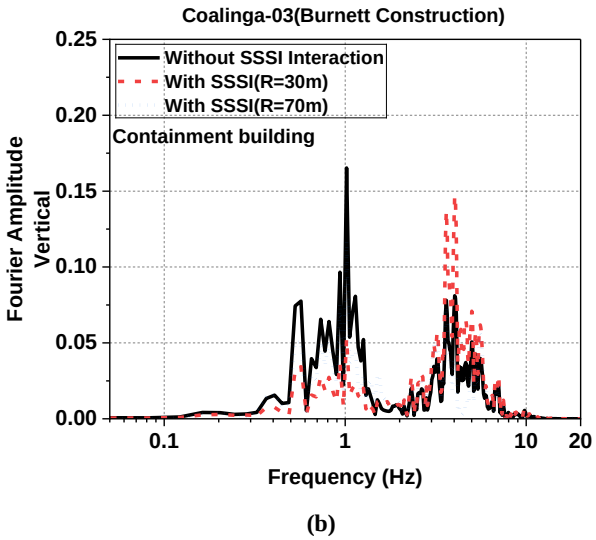


(b)

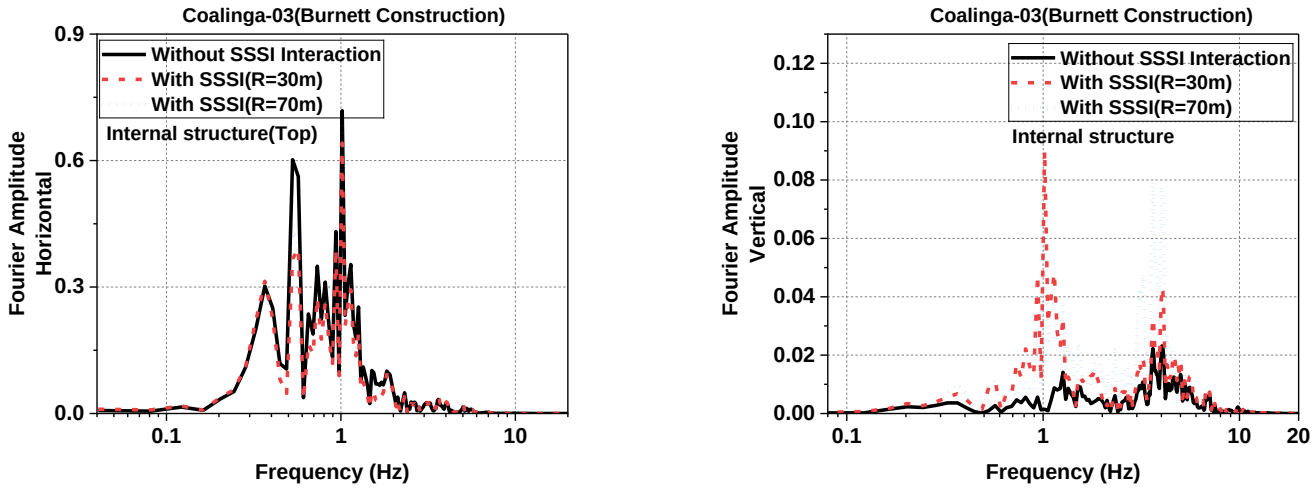


**Fig. 19. Effect of structure–soil–structure interaction (SSSI) on horizontal and vertical acceleration Fourier amplitude spectra for the containment building (a–b) and the internal structure (c–d) under unidirectional excitation of the Coalinga-03 earthquake.**

Figs. 20 and 21 illustrates the Morlet wavelet power spectra of the vertical acceleration induced by rocking motion and the horizontal acceleration at the top levels of the containment building and the internal structure, accounting for structure–soil–structure interaction (SSSI). The results indicate that SSSI does not significantly affect the time or frequency distribution of energy concentration. In the horizontal component, SSSI reduces the acceleration energy at the top of the containment building, with total energy reductions of approximately 19% and 15% for the secondary reactor modeled at 30 m and 70 m separation distances, respectively. Similarly, the horizontal-acceleration energy within the internal structure decreases by about 34% at 30 m and 26% at 70 m. Therefore, the effect of SSSI on reducing horizontal acceleration is more pronounced in the internal structure, particularly at the 30 m separation. In the vertical component, the impact of SSSI on the containment building varies across frequency ranges: for a 30 m separation, vertical acceleration energy increases by approximately 63%, whereas for a 70 m separation, vertical acceleration energy decreases by approximately 33%. Within the internal structure, vertical acceleration energy under SSSI increases by approximately 3.2 times at 30 m separation and 8 times at 70 m separation. Overall, the influence of SSSI on vertical acceleration due to rocking motion is significantly greater in the internal structure than in the containment building. The increase in vertical-acceleration energy indicates higher dynamic loading on the structure and sensitive equipment, which may lead to damage or degraded performance of structural components and systems. One of the complex and influential mechanisms affecting the seismic behavior of structures on a nuclear power plant island is the occurrence of in-phase or out-of-phase rocking. This phenomenon can significantly alter the vertical and horizontal accelerations of adjacent structures. The occurrence of in-phase or out-of-phase rocking depends on the mass and dynamic characteristics of the structures, the intensity and frequency content of the input earthquake motion, and the properties of the site soil layers [12, 34, 35]. In projects where the block-type deep soil mixing (DSM) method is employed, the simultaneous increase in mass and stiffness of the improved soil, and consequently the significant change in its dynamic impedance relative to the surrounding ground, can modify wave scattering patterns and the rocking behavior of foundations. As a result, the in-phase or out-of-phase rocking interaction between adjacent nuclear power plant structures becomes more complex. Yaghfoori et al. [14] investigated the effect of the rocking motion of the improved soil block on the surrounding ground. They demonstrated that the presence of DSM can markedly alter the distribution of vertical and horizontal accelerations. Specifically, horizontal accelerations decrease in the vicinity of the DSM block, whereas they increase farther from the improved zone. The extent of these regions and the magnitude of acceleration changes depend on the dimensions of the DSM block, the soil's dynamic properties, and the frequency content of the input ground motion. Accordingly, the spacing between adjacent structures and the relative position of each structure with respect to acceleration amplification or attenuation zones are additional key factors influencing the occurrence of in-phase or out-of-phase rocking motion in structure–soil–structure interaction (SSSI) systems. These dependencies make it difficult to draw general conclusions, underscoring the need for case-specific evaluations of SSSI effects based on each project's conditions. In the present study, the results indicate that, for both investigated spacings of 30 m and 70 m between the two nuclear power plant structures, the dominant rocking behavior is nearly out of phase. This rocking asynchrony results in only a limited reduction in horizontal accelerations in the inner structure and the containment building, while simultaneously increasing vertical accelerations in the inner structure across the entire investigated frequency range and increasing vertical accelerations in the containment building at frequencies above 2 Hz.

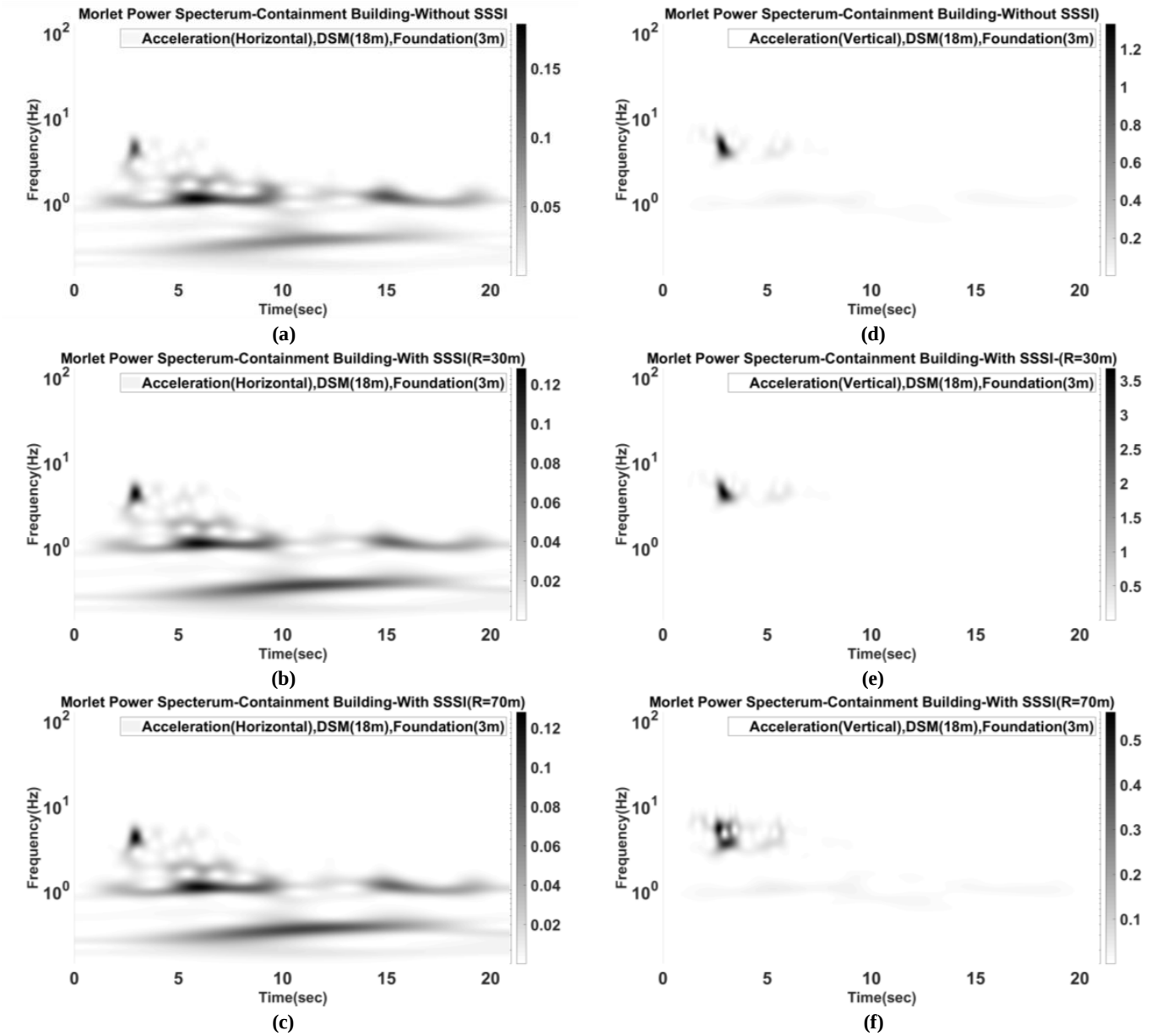


**Fig. 20. Morlet wavelet power spectrum of horizontal acceleration at the top level of the structures and vertical acceleration induced by rocking motion in the containment building, considering structure–soil–structure interaction (SSSI).**

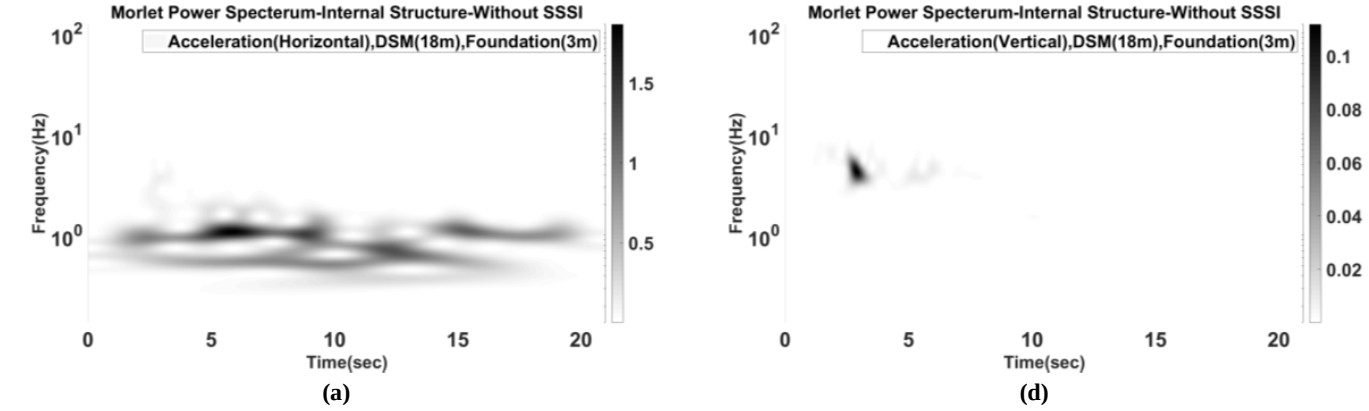

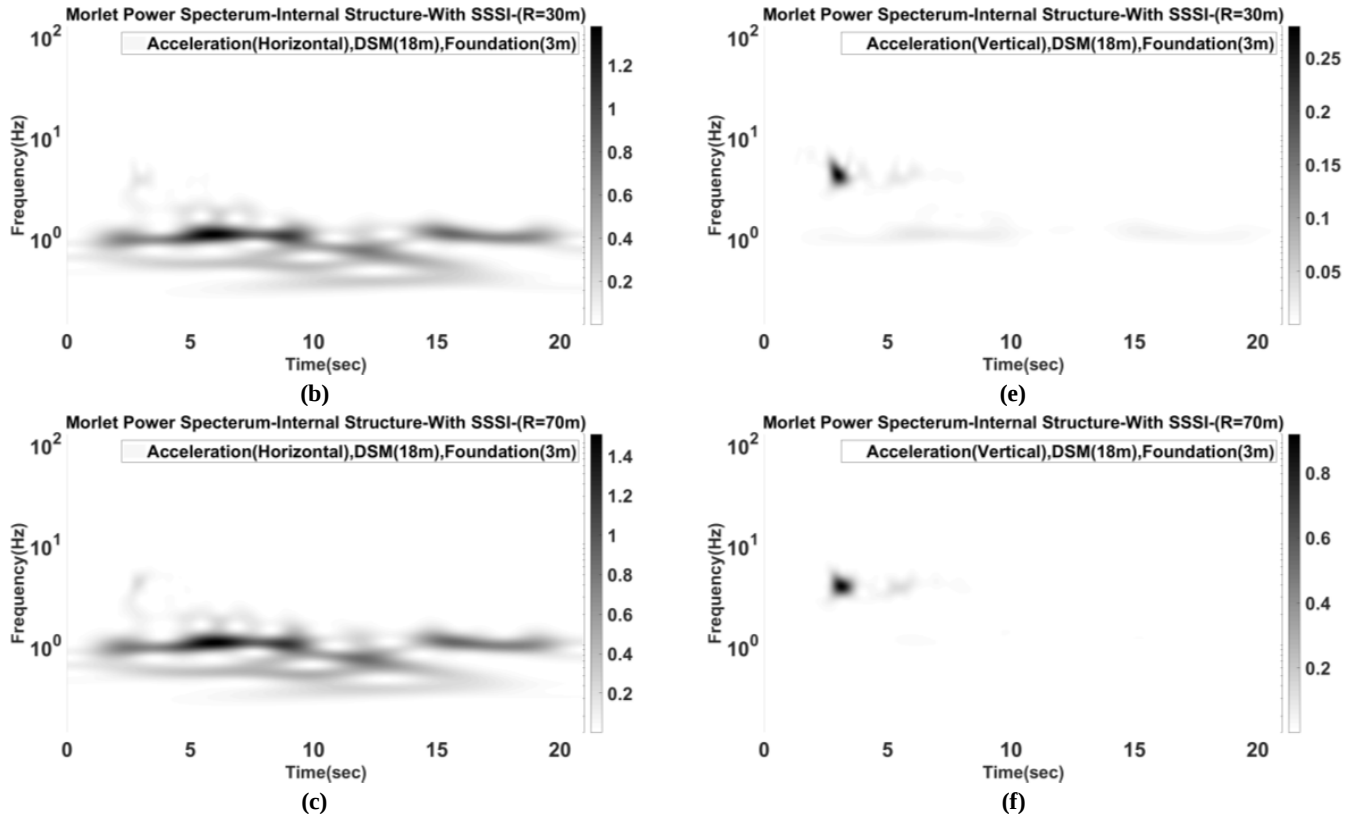


**Fig. 21. Morlet wavelet power spectrum of horizontal acceleration at the top level of the structures and vertical acceleration induced by rocking motion in the Internal Structure, considering structure–soil–structure interaction (SSSI).**

The results indicate that vertical accelerations can be significantly amplified by rocking motion under unidirectional and bidirectional loading, as well as under structure–soil–structure interaction (SSSI). This has direct implications for the Safe Shutdown Earthquake (SSE) assessment of nuclear power plants. From a regulatory and engineering perspective, the increased demand for vertical acceleration can directly affect the seismic qualification of safety-related and shutdown equipment, which is typically designed and evaluated based on vertical SSE response spectra with predefined safety margins. Amplified vertical accelerations can lead to higher axial forces, increased demands on support and anchorage systems, and local uplift at foundations and equipment bases, potentially challenging the assumed safety margins in equipment qualification. The findings of this study indicate that neglecting rocking motion, bidirectional excitation, and SSSI effects may result in a non-conservative underestimation of vertical SSE demand at both the structural and equipment levels. Consequently, the vertical acceleration transmitted to safety-critical components, including shutdown systems, may exceed design assumptions. Accordingly, this study underscores the need to explicitly account for vertical-acceleration amplification, foundation rocking, and soil–structure interaction in SSE-based seismic safety assessments, particularly for nuclear facilities on block-type DSM-improved sites. Underscores the need to explicitly account for vertical-acceleration amplification, foundation rocking, and soil–structure interaction effects in SSE-based seismic safety assessments, particularly for nuclear facilities constructed on block-type DSM-improved sites.

## 8. Limitations of the current study

The present study is subject to several modeling limitations that must be considered when interpreting the results. Due to computational constraints, the numerical analyses were performed within a two-dimensional framework; therefore, additional dynamic mechanisms, such as the torsional motion of the DSM block, which can be captured in three-dimensional models, were not considered. A lumped-mass model was used for the structural components, as permitted by ASCE 4-16 [17]. Nguyen et al. [36] also demonstrated that using a lumped-mass model provides reasonably good agreement with other reactor structural modeling approaches. Studies and technical guidelines indicate that the effects of soil–structure interaction (SSI) can differ significantly between linear and nonlinear conditions, particularly in large, stiff structures such as nuclear power plants, which exhibit multiple sources of geometric and material nonlinearity [16, 37-39]. Previous research has shown that nonlinear SSI generally reduces horizontal acceleration responses and the damping of high-frequency acceleration components due to soil plasticity [12, 15]. The primary objective of this study was to identify and interpret the dominant mechanisms of vertical acceleration amplification, particularly the roles of foundation rocking, soil–structure–structure interaction (SSSI), and block-type DSM ground improvement. For this purpose, linear elastic modeling was selected as a transparent and conservative analytical framework, allowing clear differentiation and interpretation of these mechanisms without entanglement with effects arising from material nonlinearity. Independent analyses conducted by the authors on Nevada sand, assuming elastoplastic soil behavior and block-type DSM improvement, indicate that vertical acceleration amplification due to rocking motion of the foundation is observed under both unidirectional and bidirectional loading across the predominant frequency range of the structures [28]. This suggests that the overall pattern of vertical-acceleration amplification and the governing mechanisms, particularly foundation rocking and SSI/SSSI effects, do not fundamentally change when soil nonlinearity is accounted for, although numerical response values may be adjusted.

Therefore, the reported increase in vertical accelerations within the 2–10 Hz frequency range is not solely due to the linear soil simplification but reflects the dynamic interaction of the soil–DSM–foundation–structure system. Nevertheless, for soft soils (Site Class D–F) or for conditions in which shear strains exceed approximately 0.5%, nonlinear analyses are necessary to obtain a more accurate evaluation of responses. The modeling of DSM blocks and the soil–foundation interface was also specifically addressed. DSM blocks were modeled using four-node quadrilateral elements under plane strain and with linear-elastic behavior, consistent with standard practice in the literature, in which DSM columns are typically modeled as a continuous domain with simplified material behavior [13]. The soil–structure interface is crucial for accurately modeling real-world soil–structure interaction (SSI) effects, since the foundation interacts directly with the surrounding soil at this boundary. Two main types of interfaces used in nuclear power plant analyses are tied/bonded and nonlinear/unbonded. The tied interface is the simplest, with no separation or gaps, ensuring the foundation and soil behave synchronously during dynamic events. Conversely, nonlinear interface models realistic seismic soil behavior, allowing sliding and small gaps between the foundation and the soil. This feature enables modeling of rocking motion in shallow foundations, which is essential for estimating seismic response in SSI [1]. Although nonlinear interfaces are generally believed to decrease structural seismic responses, this is not always the case. Incorrect interface specifications can lead to inaccurate seismic demand estimates, potentially compromising the safety of critical structures such as NPPs [12]. Previous research has shown that the interface's impact on structural acceleration and displacement varies with soil type and earthquake frequency. Van Nguyen et al. [15] showed that, apart from very stiff soils (S1), roof acceleration remains largely unaffected whether a fully bonded or nonlinear interface is assumed. Therefore, in most cases, nonlinear interface behavior can be ignored. However, during low- to medium-frequency earthquakes across all soil types, a sliding interface can result in greater displacements than a fully bonded interface. Sextos et al. [40] reported that containment buildings on soft soil are more susceptible to uplift and to combined nonlinear phenomena, such as sliding and rocking, particularly in response to seismic pulses in the 0.5–1.0 Hz frequency range. Saxena et al. [41, 42] further showed that sliding and gapping at the interface increase structural stresses, with the magnitude of these effects depending on the friction coefficient and the foundation embedment depth. Increasing the foundation depth can mitigate the effects of sliding and gapping. In a 3D reactor model of a 34.5 m-thick layered soil, Kanellopoulos et al. [12] demonstrated that gapping mechanisms can generate higher-frequency excitations that adversely affect internal structural components, such as the reactor containment. Therefore, the DSM–soil interface, a pivotal aspect of this study, may affect the structure's seismic response. This impact is contingent on project-specific conditions or finite-element modeling choices. However, a more robust implementation of the DSM can help alleviate these effects. Given the FE modeling conditions, substantial foundation embedment, and the DSM application, which previous studies indicate can mitigate sliding and gapping at the soil–foundation interface, along with OpenSees software limitations in the pre-processing stage, all interface nodes were tied in all directions in this study to facilitate comprehensive analyses. This study does not aim to provide a general analytical methodology covering all aspects of DSM-Soil interaction; instead, it emphasizes the importance of DSM-Soil interaction and examines the overall effect of block-type deep soil mixing, which is generally applicable.

## 9. Conclusion

This study assesses the impact of soil-structure interaction (SSI) and structure-soil-structure interaction (SSSI) on the APR1400 reactor structure, which is built on a foundation and ground enhanced through deep mixing, using laboratory results and ongoing field investigations from a power plant project. Numerical models were analyzed using three earthquake records with different frequency contents under unidirectional and bidirectional seismic excitations. The findings revealed that:

- The assessment of soil-structure interaction during unidirectional seismic events revealed that the internal structure experiences greater horizontal acceleration than the containment building. Notably, rocking in the containment causes significant vertical acceleration. The effectiveness of Deep Soil Mixing (DSM) and its interaction with both the structure and surrounding soil depend on the earthquake’s frequency content, soil dynamic properties, and DSM depth. This underscores the need for customized seismic evaluations of sensitive reactor equipment tailored to each project's specific features. Results indicate that DSM enhancements beneath the reactor foundation cause minimal changes in horizontal accelerations at high frequencies but greatly affect low-frequency responses. A key finding is the notable increase in vertical accelerations within the 2–10 Hz range, critical for many reactor components. The 18-m DSM layer increases vertical acceleration by more than 140% in the containment building and nearly 60% in the internal structure during near-fault earthquakes. These results underscore the importance of carefully evaluating DSM-improved foundations, given their substantial impact on high-frequency vertical motions.

- Analysis of the Morlet wavelet power spectra shows that the DSM layer reduces the horizontal-acceleration energy transmitted to the containment building but shifts and concentrates this energy into higher frequencies. In contrast, the 18-m BDM layer significantly amplifies vertical-acceleration energy, particularly within the 3–7 Hz frequency range, where many reactor components are most sensitive. This high-frequency concentration of vertical motion highlights the potential for increased seismic demand on nuclear structures and equipment, underscoring the need to account for DSM-induced effects in design and safety evaluations carefully.

- Near-fault ground motions notably increase vertical accelerations in both the containment building and internal structure of the APR1400 reactor, while having little impact on horizontal response. During bidirectional excitation, vertical acceleration can rise by 17–46 times for the Northridge earthquake and 6–25 times for the Coalinga earthquake, depending on the structure. These results emphasize the need to account for vertical and multidirectional excitations, as well as realistic soil–structure interaction, in the seismic design of near-fault nuclear facilities.

- The Morlet power spectrum results indicate that structure–soil–structure interaction (SSSI) does not alter the timing or

frequency bands of energy concentration but significantly affects the energy content of structural accelerations. In the horizontal component, SSSI reduces energy in both structures. For modeling the second reactor at 30 m, the reductions in the containment building and internal structure are approximately 19% and 34%, respectively, and at 70 m, 15% and 26%. In the vertical component, the influence of SSSI, particularly on the internal structure, is substantial; the vertical acceleration energy increases by about 3.2 times at 30 m and by about 8 times at 70 m. These findings highlight that SSSI can significantly amplify rocking-induced vertical demands, potentially affecting the performance and safety of structural components and sensitive equipment.

- The analysis results indicate that the vertical component of near-fault earthquakes, which typically contains high energy at high frequencies, can significantly impact the dynamic response of nuclear power plant structures. Notably, an increase in the Fourier amplitude of acceleration was observed in both the internal structure and the containment building at frequencies above 1 Hz. This becomes particularly critical, given that many mechanical and electrical equipment in such facilities exhibit high natural frequencies and are highly sensitive to excessive vertical accelerations, which may lead to functional disruption or damage. Moreover, the amplification of vertical acceleration at specific frequencies can increase axial forces in vertical members and reduce the safety margin of structural connections, thereby raising the risk of brittle failure. Relying solely on unidirectional analysis or ignoring the vertical component in seismic design can lead to inaccurate structural assessments and increased vulnerability under severe near-fault ground motions.

- The results of this study indicate that the seismic response of soil–foundation–structure systems improved with block-type DSM is highly site-specific and dependent on earthquake characteristics and structural properties; therefore, the numerical results cannot be directly generalized. Nevertheless, by focusing on the underlying physical mechanisms, the study demonstrates that factors such as the stiffness contrast between the DSM block and surrounding soil, foundation rocking, bidirectional seismic excitation, and structure–soil–structure interaction can lead to vertical acceleration amplification and redistribution of seismic energy. Although the magnitude of these effects varies by site, the mechanisms themselves are expected to be relevant to other facilities employing block-type DSM ground improvement. Accordingly, site-specific, SSI-based seismic assessments that explicitly account for DSM modeling, rocking behavior, and SSSI effects are essential for Safe Shutdown Earthquake evaluations.

## Statements & Declarations

*Author contributions*

**Ali Yaghfoori:** Conceptualization, Methodology, Software, Validation, Formal analysis, Investigation, Writing original draft, Preparation, Visualization.

**Iradj Mahmoudzadeh Kani:** Conceptualization, Methodology, Writing—review and editing, Supervision, Project administration.

**Hassan Yousefi:** Conceptualization, Methodology, Writing—review and editing, Visualization, Supervision, Project administration.

*Funding*

The authors received no financial support for the research, authorship, and/or publication of this article.

*Data availability*

The data presented in this study will be available on interested request from the corresponding author.

*Declarations*

The authors declare no conflict of interest.

## References

[1] Islam, M. R., Turja, S. D., Van Nguyen, D., Forcellini, D., Kim, D. Seismic soil-structure interaction in nuclear power plants: An extensive review. Results in Engineering, 2024; 23: 102694. doi:10.1016/j.rineng.2024.102694.

[2] Dezhkam, B., Yaghfoori, A. Soil foundation effect on the vibration response of concrete foundations using mathematical model. Computers and Concrete, 2018; 22: 221-225. doi:10.12989/cac.2018.22.2.221.

[3] Kitada, Y., Hirotani, T., Iguchi, M. Models test on dynamic structure–structure interaction of nuclear power plant buildings. Nuclear Engineering and Design, 1999; 192: 205-216. doi:10.1016/S0029-5493(99)00109-0.

[4] Yano, T., Kitada, Y., Iguchi, M., Hirotani, T., Yoshida, K. Model test on dynamic cross interaction of adjacent buildings in nuclear power plants. In: 12th world conference on earthquake engineering; 2000 30 Jan-4 Feb; Auckland, New Zealand. p. 1-8.

[5] Yano, T., Naito, Y., Iwamoto, K., Kitada, Y., Iguchi, M. Model Test on Dynamic Cross Interaction of Adjacent Building Nuclear Power Plants - Overall Evaluation on Field Test. In: Transactions of the 17th International Conference on Structural Mechanics in Reactor Technology (SMiRT 17); 2003 Aug 17–22; Prague, Czech Republic. p. 1-8.

[6] Clouteau, D., Broc, D., Devésa, G., Guyonvarh, V., Massin, P. Calculation methods of Structure–Soil–Structure Interaction (3SI) for embedded buildings: Application to NUPEC tests. Soil Dynamics and Earthquake Engineering, 2012; 32: 129-142. doi:10.1016/j.soildyn.2011.08.005.

[7] Roy, C., Bolourchi, S., Eggers, D. Significance of structure–soil–structure interaction for closely spaced structures. Nuclear Engineering and Design, 2015; 295: 680-687. doi:10.1016/j.nucengdes.2015.07.067.

[8] Lee, T. H., Wesley, D. A. Soil-structure interaction of nuclear reactor structures considering through-soil coupling between adjacent structures. Nuclear Engineering and Design, 1973; 24: 374-387. doi:10.1016/0029-5493(73)90007-1.

[9] Bolisetti, C., Whittaker, A. Seismic structure–soil–structure interaction in nuclear power plant structures. In: 21st International Conference on Structural Mechanics in Reactor Technology (SMiRT 21); 2011 Nov 6-11; New Delhi, India. p. 6-11.

[10] Yue, D., Ghiocel, D. M., Fuyama, H., Ogata, T., Stark, G. Structure-soil-structure interaction effects for two heavy NPP buildings with large-size embedded foundations. In: 22nd International Conference on Structural Mechanics in Reactor Technology (SMiRT22); 2013 Aug 18-23; San Francisco, California. p. 18-23.

[11] Anderson, L. M., Carey, S., Amin, J. Effect of Structure, Soil, and Ground Motion Parameters on Structure-Soil-Structure Interaction of Large Scale Nuclear Structures. Structures Congress, 2012; 2862-2873. doi:10.1061/41171(401)249.

[12] Kanellopoulos, C., Rangelow, P., Jeremic, B., Anastasopoulos, I., Stojadinovic, B. Dynamic structure-soil-structure interaction for nuclear power plants. Soil Dynamics and Earthquake Engineering, 2024; 181: 108631. doi:10.1016/j.soildyn.2024.108631.

[13] Shaghaghi, M. M., Kani, I. M., Yousefi, H. The Seismic Behavior of Block Type Deep Soil Mixing. Latin American Journal of Solids and Structures, 2021; 18: 1-17. doi:10.1590/1679-78256439.

[14] Yaghfoori, A., Mahmoudzadeh Kani, I., Yousefi, H. Seismic performance and optimization of deep soil mixing (DSM) for response mitigation at power plant sites. Engineering Computations, 2025; 1-42. doi:10.1108/EC-05-2025-0508.

[15] Van Nguyen, D., Kim, D., Duy Nguyen, D. Nonlinear seismic soil-structure interaction analysis of nuclear reactor building considering the effect of earthquake frequency content. Structures, 2020; 26: 901-914. doi:10.1016/j.istruc.2020.05.013.

[16] Bolisetti, C., Whittaker, A. S., Coleman, J. L. Linear and nonlinear soil-structure interaction analysis of buildings and safety-related nuclear structures. Soil Dynamics and Earthquake Engineering, 2018; 107: 218-233. doi:10.1016/j.soildyn.2018.01.026.

[17] (ASCE), A. S. o. C. E. Seismic analysis of safety-related nuclear structures. 1st ed. Reston (VA): American Society of Civil Engineers (ASCE); 2017. doi:10.1061/9780784413937.

[18] Jeremić, B., Jie, G., Preisig, M., Tafazzoli, N. Time domain simulation of soil–foundation–structure interaction in non-uniform soils. Earthquake Engineering & Structural Dynamics, 2009; 38: 699-718. doi:10.1002/eqe.896.

[19] Amalu, P. A., Jayalekshmi, B. R. Study on seismic response of unconnected piled raft with rubber mixed soil. Materials Today: Proceedings, 2023; doi:10.1016/j.matpr.2023.10.018.

[20] Çetindemir, O., Zülfikar, A. C. Numerical validation of fully coupled nonlinear seismic soil–pile–structure interaction. Buildings, 2024; 14: 1502. doi:10.3390/buildings14061502.

[21] Cruz, L., Todorovska, M. I., Chen, M., Trifunac, M. D., Aihemaiti, A., Lin, G., Cui, J. The role of the foundation flexibility on the seismic response of a modern tall building: Vertically incident plane waves. Soil Dynamics and Earthquake Engineering, 2024; 184: 108819. doi:10.1016/j.soildyn.2024.108819.

[22] Nielsen, A. H. Absorbing boundary conditions for seismic analysis in ABAQUS. In: ABAQUS users' conference; 2006 May 23-25; Cambridge, Massachusetts. p. 359-376.

[23] Rathje, E. M., Faraj, F., Russell, S., Bray, J. D. Empirical relationships for frequency content parameters of earthquake ground motions. Earthquake Spectra, 2004; 20: 119-144. doi:10.1193/1.1643356.

[24] Tso, W. K., Zhu, T. J., Heidebrecht, A. C. Engineering implication of ground motion A/V ratio. Soil Dynamics and Earthquake Engineering, 1992; 11: 133-144. doi:10.1016/0267-7261(92)90027-B.

[25] Patrício, J. D., Gusmão, A. D., Ferreira, S. R. M., Silva, F. A. N., Kafshgarkolaei, H. J., Azevedo, A. C., Delgado, J. M. P. Q. Settlement Analysis of Concrete-Walled Buildings Using Soil–Structure Interactions and Finite Element Modeling. Buildings, 2024; 14: 746. doi:10.3390/buildings14030746.

[26] Uzun, S., Ayvaz, Y. Implementation of PMDL and DRM in OpenSees for Soil-Structure Interaction Analysis. Applied Sciences, 2024; 14: 8519. doi:10.3390/app14188519.

[27] Towhata, I. Geotechnical earthquake engineering: Damage mechanism observed. 1st ed. Berlin (DE): Springer International Publishing;; 2015. doi:10.1007/978-3-642-35344-4_2.

[28] Yaghfoori, A., Mahmoudzadeh Kani, I., Yousefi, H. Seismic behavior of dry sandy soils improved with Block-Type Deep Soil Mixing in near-fault regions. AUT Journal of Civil Engineering, 2025; doi:10.22060/ajce.2025.24157.5923.

[29] Asgari, A., Ranjbar, F., Bagheri, M. Seismic resilience of pile groups to lateral spreading in liquefiable soils: 3D parallel finite element modeling. Structures, 2025; 74: 108578. doi:10.1016/j.istruc.2025.108578.

[30] Asgari, A., Sorkhi, S. F. A. Wind turbine performance under multi-hazard loads: Wave, wind, and earthquake effects on liquefiable soil. Results in Engineering, 2025; 26: 104647. doi:10.1016/j.rineng.2025.104647.

[31] Chopra, A. K., Chintanapakdee, C. Comparing response of SDF systems to near-fault and far-fault earthquake motions in the context of spectral regions. Earthquake Engineering & Structural Dynamics, 2001; 30: 1769-1789. doi:10.1002/eqe.92.

[32] Bozorgnia, Y., Campbell, K. W. The vertical-to-horizontal response spectral ratio and tentative procedures for developing simplified V/H and vertical design spectra. Journal of Earthquake Engineering, 2004; 8: 175-207. doi:10.1080/13632460409350486.

[33] Tyapin, A. Effect of soil improvement on seismic response. In: 24th International Conference on Structural Mechanics in Reactor Technology (SMiRT 24 ); 2017 Aug 20-25; Busan, Korea. p. 1-10.

[34] Lu, X., Jing, L., Ma, Y., Yang, J., Qi, W. Shaking table test for seismic response of nuclear power plant on non-rock site. Sustainability, 2023; 15: 10366. doi:10.3390/su151310366.

[35] Anagnostopoulos, S. A., Spiliopoulos, K. V. An investigation of earthquake induced pounding between adjacent buildings. Earthquake Engineering & Structural Dynamics, 1992; 21: 289-302. doi:10.1002/eqe.4290210402.

[36] Nguyen, D.-D., Thusa, B., Park, H., Azad, M. S., Lee, T.-H. Efficiency of various structural modeling schemes on evaluating seismic performance and fragility of APR1400 containment building. Nuclear Engineering and Technology, 2021; 53: 2696-2707. doi:10.1016/j.net.2021.02.006.

[37] Lee, J. H. Practical Numerical Approach for Nonlinear Soil-Structure Interaction Analysis of a NPP Containment Building. In: Transactions of the Korean Nuclear Society Spring Meeting; 2018 May 17-18; Jeju, Korea. p. 1-2.

[38] Kabanda, J., Kwon, O.-S., Kwon, G. Time and frequency domain analyses of the Hualien Large-Scale Seismic Test. Nuclear Engineering and Design, 2015; 295: 261-275. doi:10.1016/j.nucengdes.2015.10.011.

[39] Asgari, A. Effect of Deep Soil Mixing Grid on the Reduction Coefficient in the Liquefiable Soil: 3D Nonlinear Modeling. Journal of Civil and Environmental Engineering, 2025; 55: 89-98. doi:10.22034/ceej.2025.63522.2381.

[40] Sextos, A. G., Manolis, G. D., Athanasiou, A., Ioannidis, N. Seismically induced uplift effects on nuclear power plants. Part 1: Containment building rocking spectra. Nuclear Engineering and Design, 2017; 318: 276-287. doi:10.1016/j.nucengdes.2016.12.035.

[41] Saxena, N., Paul, D., Kumar, R. Effects of slip and separation on seismic SSI response of nuclear reactor building. Nuclear Engineering and Design, 2011; 241: 12-17. doi:10.1016/j.nucengdes.2010.10.011.

[42] Saxena, N., Paul, D. K. Effects of embedment including slip and separation on seismic SSI response of a nuclear reactor building. Nuclear Engineering and Design, 2012; 247: 23-33. doi:10.1016/j.nucengdes.2012.02.010.